Fatigue Life of High-Strength Steel Offshore Tubular Joints

Petersen, R. I.; Agerskov, H.; Lopez Martinez, L.

Publication date:
1996

Document Version
Publisher's PDF, also known as Version of record

Institut for Bærende Konstruktioner og Materialer
Department of Structural Engineering and Materials
Danmarks Tekniske Universitet • Technical University of Denmark

BKM

Fatigue Life of High-Strength Steel Offshore Tubular Joints

R.I. Petersen, H. Agerskov & L. Lopez Martinez

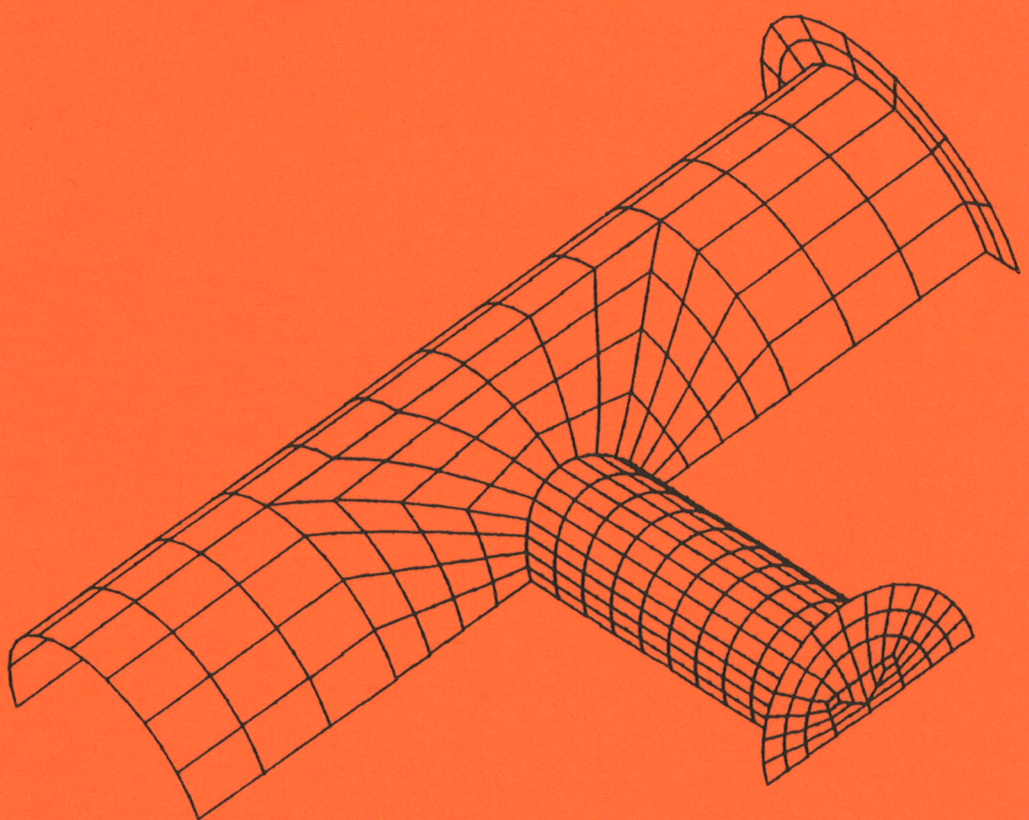

Serie R No 1 1996

FATIGUE LIFE OF HIGH-STRENGTH STEEL OFFSHORE TUBULAR JOINTS

by

R.I. PETERSEN[1)], H. AGERSKOV[1)] & L. LOPEZ MARTINEZ[2)]

[1)] Department of Structural Engineering and Materials, Technical University of Denmark, Lyngby, Denmark
[2)] Research and Development, Svenskt Stål AB, Oxelösund, Sweden

Fatigue Life of High-Strength Steel Offshore Tubular Joints

Tryk:
LTT
Danmarks Tekniske Universitet
Lyngby
ISBN 87-7740-167-0
ISSN 1396-2167
Bogbinder:
H. Meyer, Bygning 101, DTU

CONTENTS

SYNOPSIS

In the present investigation, the fatigue life of tubular joints in offshore steel structures is studied. Two test series on full-scale tubular joints have been carried through. One series was on joints in conventional offshore structural steel, and the other series was on joints in high-strength steel with a yield stress of 820-830 MPa and with high weldability and toughness properties. The test specimens of both series had the same geometry. The present report concentrates on the results obtained in the investigation on the high-strength steel tubular joints.

The test specimens were fabricated from Ø 324-610 mm tubes, and the joints were loaded in in-plane bending. Both fatigue tests under constant amplitude loading and tests with a stochastic loading that is realistic in relation to offshore structures, are included in the investigation.

A comparison between constant amplitude and variable amplitude fatigue test results showed shorter fatigue lives in variable amplitude loading than should be expected from the linear fatigue damage accumulation formula. Furthermore, the fatigue tests on high-strength steel tubular joints showed slightly longer fatigue lives than those obtained in corresponding tests on joints in conventional offshore structural steel.

1. INTRODUCTION

In the North Sea, a large number of offshore steel structures has been constructed over the last three decades. Soon after oil and gas exploration and production began in the North Sea in the mid 1960'es, it became apparent that the steel structure design developed for offshore activities in the Gulf of Mexico was not adequate, when transferred to the more rigorous North Sea environment. In particular, fatigue cracks evolved as a result of wave action during severe winter storms. Thus, it was evident that there was a great need for better understanding of the fatigue phenomenon, so that safer structures could be built.

This lack in the understanding of the fatigue behaviour of offshore steel structures has resulted in comprehensive investigations carried out both in Scandinavia and on a wider European basis, involving all the countries located around the North Sea.

In the Danish part of the North Sea with oil and gas production, water depths are rather moderate, around 40-60 m, but frequent storms also create a rough environment in this area. At present, the Danish oil and gas fields in the North Sea have a total of about 35 fixed steel platforms.

One of the problems in the design of offshore steel structures that has attracted increased attention in recent years is the problem of fatigue damage accumulation. Codes and specifications normally give simple rules, using a Miner summation and based on the results of constant amplitude fatigue tests, [7,10,12,13]. However, the actual load situations for offshore structures deviate considerably from simple constant amplitude loading, and the need for a better understanding of the fatigue behaviour under more realistic fatigue loading conditions is obvious.

Over the last few years, very interesting new high-strength steels with high weldability and toughness properties have been developed and come into production. Due to the possibilities of weight savings, these steel types are also interesting in offshore applications, and their fatigue behaviour when used in structural elements needs to be clarified.

In the present investigation, the fatigue life of high-strength steel tubular joints in offshore

structures is studied. This investigation is a part of a series of research projects on fatigue in offshore steel structures, carried out at the Department of Structural Engineering of the Technical University of Denmark. The primary purpose of these projects is to study the fatigue life of offshore steel structures under various types of stochastic loading that are realistic in relation to offshore structures.

The experimental investigation comprises both test series on full-scale tubular joints and test series on smaller welded test specimens. However, due to the high costs of the full-scale tubular joint test specimens, the large number of fatigue tests in these investigations is carried out on the smaller welded plate test specimens, and only a limited number of tests on the full-scale tubular joints is carried out to check that the main results, concerning fatigue damage accumulation, obtained in the test series on the plate specimens are also valid for the tubular joints.

The materials used in the present investigation in the fabrication of the test specimens are high-strength steels with a yield stress of ~ 800-1000 MPa, and with high weldability and toughness properties. However, a similar investigation has been carried out with test specimens in conventional offshore structural steel with a yield stress of ~ 360-410 MPa, see Agerskov and Ibsø, [4,19].

In the load simulation in the fatigue tests with variable amplitude loading, a one-step Markov model is used. Both narrow-banded and broad-banded spectra, with irregularity factors ranging from ~ 0.70 to 1.00 have been investigated. Instrumentation and testing techniques comprise e.g. determination of stress distributions by use of thermoelastic stress analysis technique (SPATE) and strain gages, in combination with finite element analysis. Fatigue crack propagation is determined by use of AC-potential drop technique.

This report presents the results that have been obtained in the investigation on the high-strength steel tubular joints.

2. EXPERIMENTAL INVESTIGATION

2.1 Experiment Design and Test Specimens

The experimental investigation comprises test series on full-scale tubular joints as well as test series on smaller welded plate test specimens.

The dimensions that have been chosen for the tubular joints, see Fig. 2.1, correspond to a large number of the joints in the platforms of the Tyra Field in the North Sea. Compared with the largest joints in these platforms, the actual test joints are approximately half size. The Tyra Field is, with 9 fixed platforms, one of the biggest Danish oil and gas fields.

The test specimens are carried out as double T-joints. This gives for each test specimen four critical areas with respect to fatigue cracks, since these may be expected to develop at the edges of the weld between the main tube and the secondary tube, in or near the symmetry

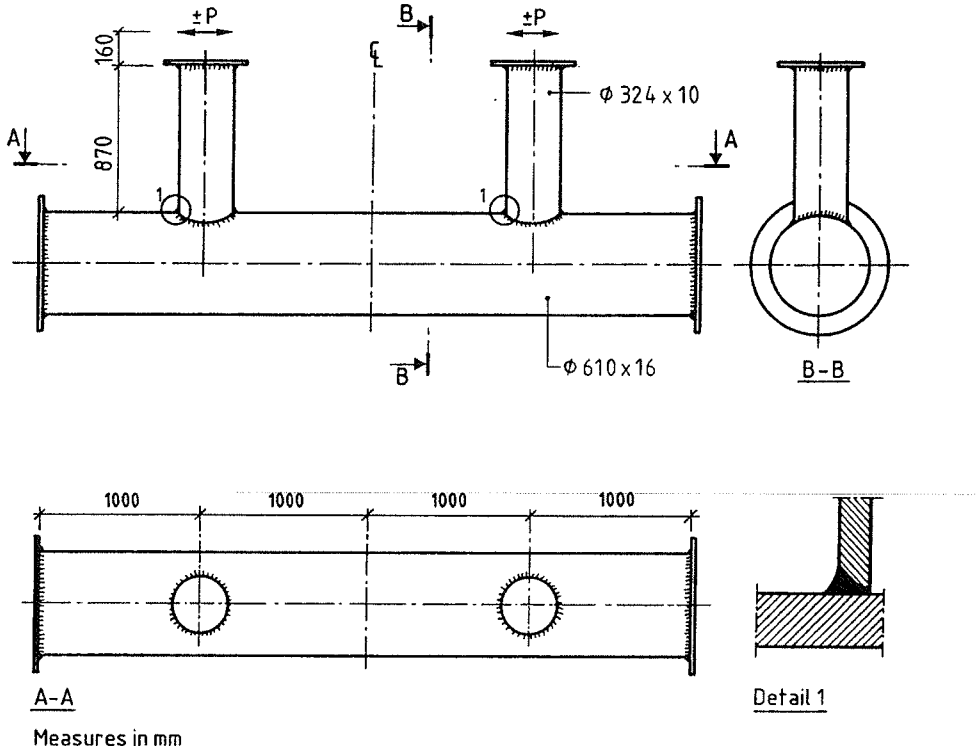

Fig. 2.1 Tubular joint test specimen.

plane of the test specimen. The test joint is loaded in in-plane bending, as may be seen in Fig. 2.1. Each test series comprises three test specimens with two tubular joints in each of them.

In the investigation on joints in conventional offshore structural steel, the materials used, as well as the welding procedures, the quality of the welding, and the control of the welding were identical to those used in the platforms of the Tyra Field. The material quality of both main tube and secondary tube is API 5LX GR.X-52N with a yield stress of f_y = 363-381 MPa and an ultimate tensile strength, f_u = 506-548 MPa. Details of the materials and the welding of the joints may be found in Ref. 18.

After the first series of fatigue tests on the tubular joints in conventional offshore structural steel, the fatigue cracks in the joints were repair-welded, and the fatigue tests were repeated. In the repair-welding, it has been emphasized that the welding procedures correspond as precisely as possible to procedures used presently in the North Sea in repair-welding of fatigue cracks in tubular structures. The procedures were worked out in cooperation with Det Norske Veritas. After both series of tests had been carried through, the fatigue life of the repair-welded tubular joints could be compared with the fatigue life of the original joints. The results obtained in this investigation are given in Ref. 3.

The test series on the smaller welded joints are carried out on test specimens, which consist of a 40 or 90 mm wide main plate with two transverse secondary plates welded to the main plate by means of full penetration butt welds. This also gives four critical areas with respect to fatigue for these test specimens, since the fatigue crack will initiate at the edge of the weld and propagate into the main plate. Two different dimensions are used for these test specimens, to study the size effect. The applied loading in these tests is a central normal force in the main plate. The test specimens are shown in Fig. 2.2.

The material used for the plate test specimens in high-strength steel is Weldox 700. All plates were manufactured by Svenskt Stål AB, Oxelösund, Sweden. The plates have a yield stress of f_y = 810-840 MPa, and an ultimate tensile strength, f_u = 845-875 MPa. For the plate test specimens in conventional offshore structural steel, f_y = 400-409 MPa and f_u = 537-575 MPa.

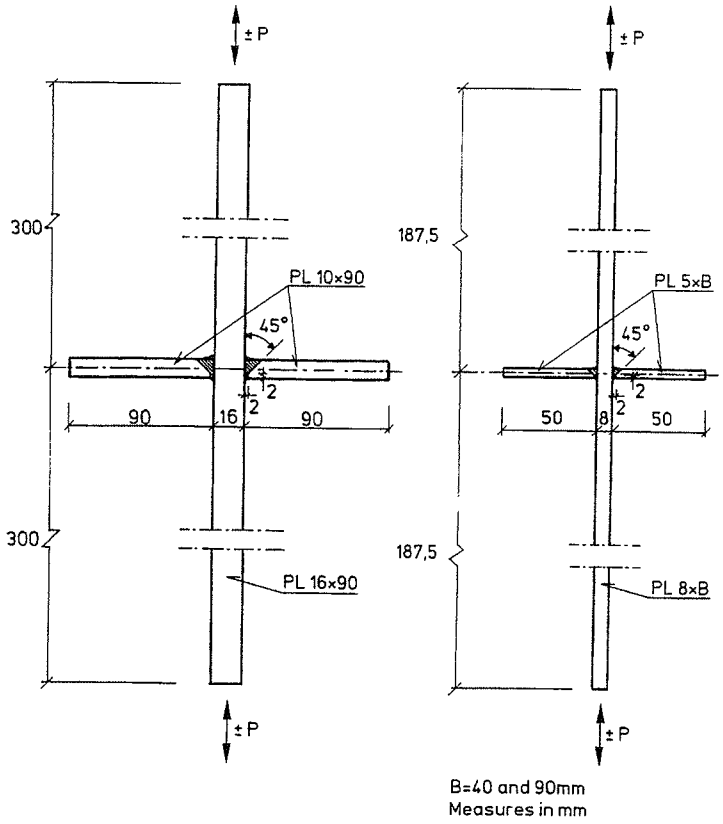

Fig. 2.2 Welded plate test specimens with transverse attachments.

Details of the materials and the fabrication of the welded plate test specimens may be found in Refs. 18, 28 and 29.

2.2 Materials of Tubular Joint Test Specimens

The tubular joint test specimens in high-strength steel have been fabricated from plates which have been formed to tubes by rolling bending process. The material quality of both main tube and secondary tube is Weldox 700.

Weldox 700 is a quenched and tempered high-strength steel. All the plates were manufactured by Svenskt Stål AB, Oxelösund, Sweden. The chemical composition and mechanical properties are given in Tables 2.1 and 2.2, respectively.

The Charpy V-notch tests for the plates were carried out at a temperature of -40° C. Longitudinal direction test specimens were used for both plate thicknesses. The results of the Charpy V-notch tests are presented in Table 2.3. The values presented are the mean values from 8 different tests.

Thickness (mm)	C	Si	Mn	P	S	Mo	V	Ti
16	0.15	0.44	1.32	0.012	0.002	0.099	0.060	-
10	0.13	0.47	1.44	0.014	0.001	0.003	0.060	0.030

Thickness (mm)	Al	Nb	B	N_{max}	H_{max}	CE_{IIW}	P_{cm}
16	0.060	0.025	0.002	0.008	-	0.41	0.258
10	0.030	0.025	0.002	0.008	-	0.37	0.232

Table 2.1 Chemical composition for steel plates used in test specimens.

Thickness (mm)	Yield stress (MPa)	Ultimate tensile strength (MPa)	A_5 (%)
16	830	863	14.5
10	823	853	16

Table 2.2 Mechanical properties of steel plates used in test specimens.

Thickness (mm)	Temperature (°C)	Specimen type	Individual tests (J)	Mean value (J)
10	-40	5x10	45,47,54	49
16	-40	5x10	104,110,120	111
16	-40	5x10	125,106,113	115

Table 2.3 Results of Charpy V-notch tests for steel plates used in test specimens.

2.3 Fabrication of Tubular Joint Test Specimens

The dimensions of the test specimens are shown in Fig. 2.1. After rolling bending to the correct diameters, the plates were welded to tubes according to the weld procedure given in Table 2.4. The number of passes was 4. For the first pass, the filler metal used was OK 48.00 and for the rest, OK 78.12, see Fig. 2.3.

The weld parameters used for the welded joint between main tube and secondary tube may also be found in Table 2.4. The number of passes in this case was 10, and for all the passes the same filler metal, OK 78.12, was used.

Filler metal	Weld method	Num-ber of passes	Weld posit.	Electr. diam. (mm)	Current (A)	Voltage (V)	Heat input (kJ/mm)	Inter-pass temp.
OK 48.00	SMAW	1	1 G	3.25	90-140	23	2.0	-
OK 78.12	SMAW	2-10	1 G	4 & 5	110-180 170-240	24 & 25	1.6	Max. 250 °C

Table 2.4 Weld procedures for tubular joints.

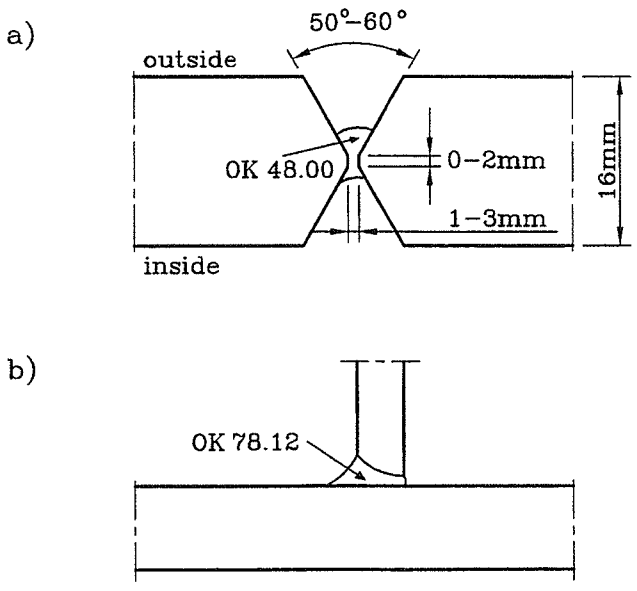

Fig. 2.3 a) Welded joint in main tube.
b) Welded joint between main tube and secondary tube.

The test specimens were fabricated by one of the Swedish steel contractors, Uddcomb Engineering, well experienced in the fabrication of steel structures. The longitudinal welds in the main tube and in the secondary tubes were placed in the test specimens in such a way that they would not interfere with the fatigue cracks.

In Table 2.5 are given the chemical composition and mechanical properties of the filler metal used in the welding of the tubular joint test specimens.

	OK 48.00	OK 78.12
C	0.07	0.04-0.08
Si	0.5	0.20-0.50
Mn	1.2	1.30-1.80
P	0.025	0.020
S	-	0.020
Mo	-	0.30-0.50
Ni	-	1.80-2.50
Yield stress (MPa)	455	680-760
Ultimate tensile strength (MPa)	540	760
A_5(%)	29	20(A_4)
Impact Charpy-V	-20°C: 160J -40°C: 80J	-51°C: 47J

Table 2.5 Chemical composition and mechanical properties of filler metal used in welding of tubular joint test specimens.

2.4 Control of Tubular Joint Test Specimens

As the full-scale tubular joint test specimens were fabricated without preheat, a complete ultrasonic examination and magnet particle inspection was carried out on the welded joints, where fatigue cracks were expected. The purpose of this examination was primarily to ensure that no cold cracks were present before fatigue testing. The examination was carried out by the Force Institutes, Copenhagen, [15].

The magnet particle inspections revealed no surface cracks on any of the tubular joints. The ultrasonic examination detected inclusions at points located at the inside of the weldings. These defects are presumed to originate from stitch weldings used at the initial stages of the welding process. As all fatigue cracks developed on the outside of the weldings away from the detected inclusions, the fatigue properties of the tubular joints were not affected by these defects.

2.5 Test Equipment and Test Procedure

2.5.1 Test Equipment

Three sets of equipment for fatigue testing have been built up in connection with the present project. Each set consists of an actuator, a servo-controller, and a computer, with two of the actuators having one servo-controller in common. All three actuators are supplied from a common pump station. An overview of the fatigue test equipment is shown in Fig. 2.4.

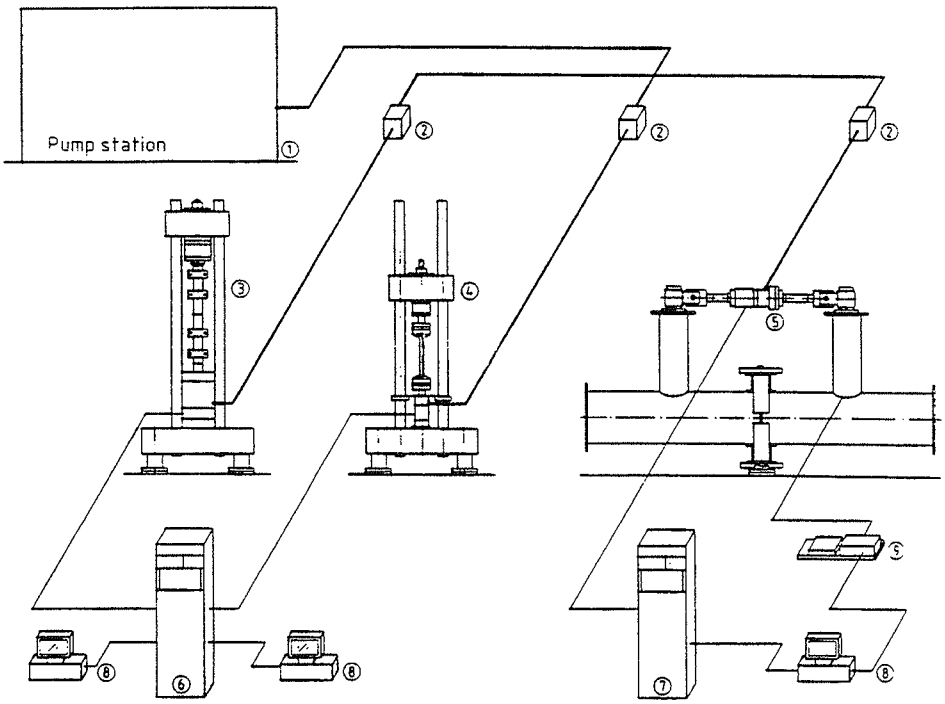

Fig. 2.4 Overview of fatigue test equipment. The figure shows: (1) Pump station, (2) Sub-stations, (3) 500 kN actuator, (4) 100 kN actuator, (5) 125 kN actuator, (6) and (7) Servo-controllers, (8) Computers, and (9) Crack depth measuring equipment, [2].

In the test equipment, one actuator, No. 3 in Fig. 2.4, has a capacity of ± 500 kN dynamic loading and a stroke of ± 30 mm. It is intended for testing larger plate test specimens under axial loading. Actuator No. 4 has a capacity of ± 100 kN dynamic loading and a stroke of ± 28 mm. It is intended for testing smaller plate test specimens under axial loading. Finally, actuator No. 5 has a capacity of ± 125 kN dynamic loading and a stroke of ± 50 mm. This test setup has been designed specifically for in-plane bending tests with tubular joint test specimens, as indicated in Fig. 2.4.

A more detailed description of the test equipment may be found in Ref. 27.

Strain gages are used to determine the stresses in the test specimens. This includes determination of the hot spot stresses in both main tube (chord) and secondary tube (branch), as well as the stress distribution along the main tube in the symmetry plane and stresses in a number of points near the joint.

Furthermore, the stresses in the most critical areas with respect to fatigue have been determined from finite element analysis and by use of thermoelastic technique (SPATE). This is an experimental stress analysis technique based on the measurement of infrared radiant flux emitting from the surface of a body under cyclic stress, see e.g. Refs. 8, 31 and 32. Fatigue crack propagation during the test is determined by use of AC-potential drop technique. A computer is used to store sequences of recorded maxima and minima.

A number of computer programs have been developed to control experiments, to perform data sampling, and for treatment of test data. The most important of these programs are described in detail in Ref. 1.

2.5.2 Test Procedure for Tubular Joints

The test arrangement used in the investigation on the tubular joints may be seen in Fig. 2.5. The test joint is loaded in in-plane bending.

The test specimen is fixed by use of a prestressed glulam clamp in the symmetry plane perpendicular to the main tube, whereas the rest of the test specimen is free to move. This

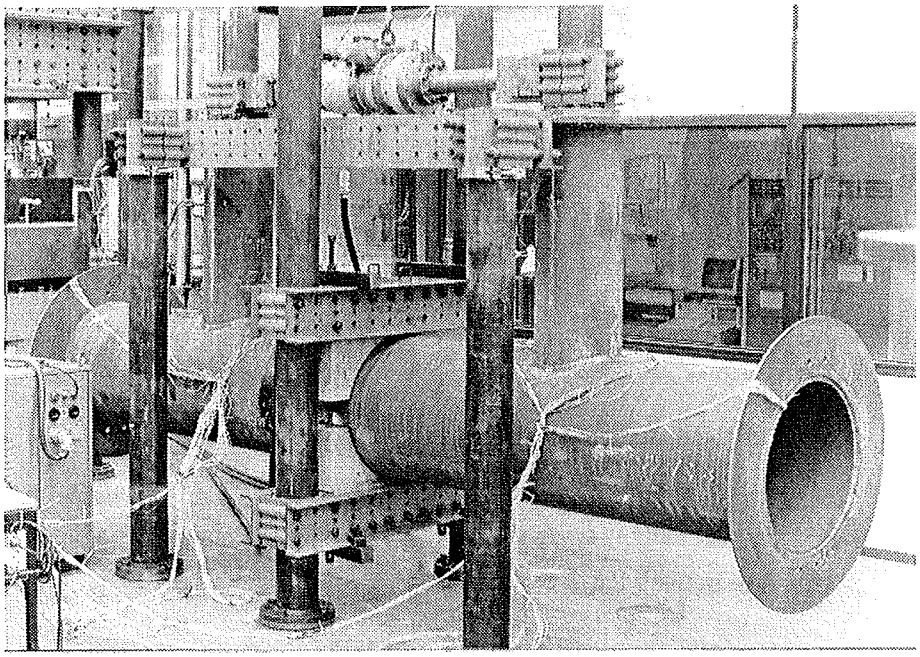

Fig. 2.5 Test arrangement in investigation on full-scale double T-joint.

is not a very stiff support, but due to the symmetry in both geometry and loading, this support is adequate. The tube will behave as if a fixed support was present in the symmetry plane.

The actuator is mounted directly on the test specimen to obtain perfect symmetry in the loading. The weight of the actuator is outbalanced by suspension in a single spring. The mounting of the actuator in the tubular joint tests may be seen in Fig. 2.5.

When the fatigue crack at the weld between the main tube and one of the secondary tubes has reached a prescribed length, the test is stopped. The remaining part of the fatigue test is carried out, using a stiffening arrangement between the end of the main tube and the end of the branch, at the end of the test specimen where the crack has developed, cf. Fig. 2.6. This arrangement makes it possible to continue the fatigue test until the final crack length is also reached at the other end, without further crack growth at the stiffened end.

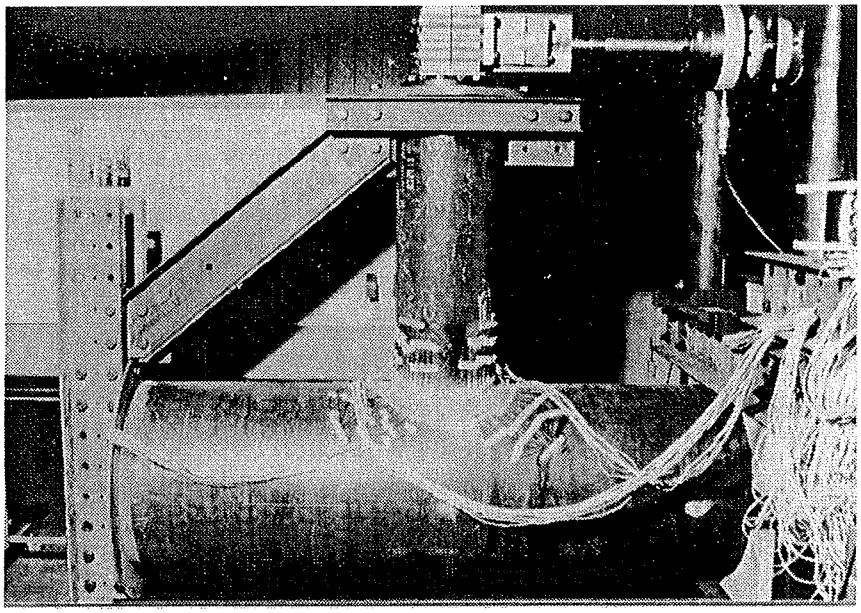

Fig. 2.6 Stiffening arrangement in fatigue tests on tubular joints.

Since fatigue cracks are present - and growing - during a considerable part of the total fatigue life, it is important to establish a criterium for the crack size, at which the test is stopped. The criterium that has been chosen in the present investigation is a through crack in the chord wall, with an inside length of 120-150 mm, or a crack in the branch with an outside length of ~ 340 mm. Both criteria correspond to a fatigue crack developed on the outside over about 120^{o} along the perimeter of the branch at the toe of the weld. At this stage, the crack growth is very fast, and thus the number of cycles to "failure" is well defined.

Two equally loaded branches yield 8 critical points with respect to fatigue crack development, since the cracks may be expected to develop at the edges of the weld between the main tube and the branch. At each point, at least two axial strains are needed to calculate the hot spot stress. To determine the stresses in the plane stress state in the critical regions, also the tangential strains are measured. This gives a minimum of 32 strain gage measurements in the fatigue tests. Since the cracks will change the stress state, these measurements are taken in the beginning of the test, before any crack development has started.

In the stochastic loading tests, a sequence of peaks from approx. 10000 cycles are filed for each of the 32 strain gages. 10000 cycles have proven to give a reliable equivalent stress

range. A more detailed description of the strain gage measurements is given in chapter 3. Fig. 2.7 shows the strain gage instrumentation for determination of the hot spot stresses in chord and brace.

The fatigue tests on the tubular joints have been carried out at a relatively high load level. In the constant amplitude tests, a loading of P = ± 30 kN was used, and in the stochastic loading tests, the maximum value of the load was P_{max} = ± 57.5 kN. These load levels correspond to equivalent hot spot stress ranges of approx. 150-200 MPa. It was found that an average frequency of about 3-5 Hz was appropriate for these tests.

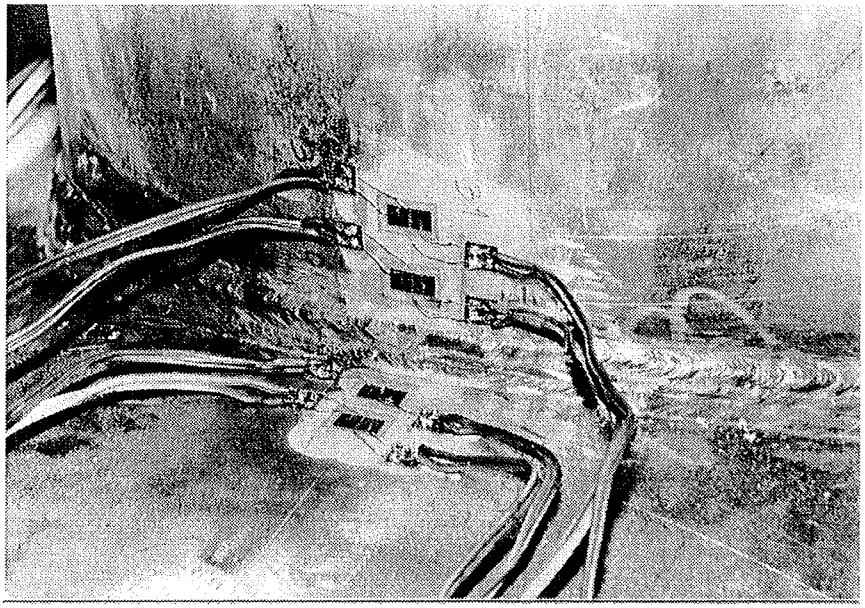

Fig. 2.7 Strain gage instrumentation for determination of hot spot stresses. Test No. W1.

2.6 Variable Amplitude Loading

As mentioned previously, fatigue design curves have traditionally been obtained from constant amplitude tests. This, however, is not realistic in relation to wave action, which is the dominant variable loading on offshore structures. One of the main aims of this project is to carry through both test series and analytical investigations to study the differences between fatigue life under variable amplitude loading, realistic to offshore structures, and constant amplitude loading.

There is a number of ways to simulate stochastic processes in fatigue testing. The approach that has been chosen in the present investigation is the Markov matrix method. The variable amplitude loading is generated by a computer program "Tantalus", developed at the Department of Structural Engineering of the Technical University of Denmark, [1]. The program simulates a stationary Gaussian stochastic process in real time.

The load history used in the tests represents a stationary process, which does not directly correspond to a long term wave distribution. However, for each of the load spectra investigated, the different load levels, i.e. different equivalent stress ranges, will correspond to different sea states. Thus, the fatigue tests in each test series will give information about the fractional fatigue damage accumulation in the various sea states that form the total long term wave distribution.

2.6.1 The Markov Matrix

The method is applicable to simulation of stationary processes, that is, the wave action is divided into a number of sea states, in which the load can be described by a stationary stochastic process.

The Markov model only provides extreme values in the load history; the load course between consecutive extremes is considered to be without importance. This enables use of a fast simulation algorithm.

The method has a one-step memory, having an extreme $a^{\ell-1}$, the next extreme a^{ℓ} is generated only with knowledge of $a^{\ell-1}$, and without any dependence on previous extremes. The simulation is controlled through the Markov matrix. The total load range is divided into a discrete number of load levels, n_m (typically 32 or 64), which corresponds to the size of the two-dimensional Markov matrix. Each column and each row in the matrix corresponds to a load level, and the matrix elements contain cumulated transition probabilities, that is, element p_{ij} is the probability that the next load level is less than level i, given that the present load level is level j, or:

$$p_{ij} = P\{a^{\ell} < a_i \mid a^{\ell-1} = a_j\} \qquad (2.1)$$

The actual matrix element to be chosen, given a certain load level, is determined by use of a random number generator, as shown in principle in Fig. 2.8.

When the process is symmetric with respect to zero, only a triangular matrix is necessary. If the upper triangle is chosen, only maxima are generated, and minima are obtained by changing sign on every other maximum.

The control principle and the documentation of the controlling computer program is described in detail by Aarkrog, [1].

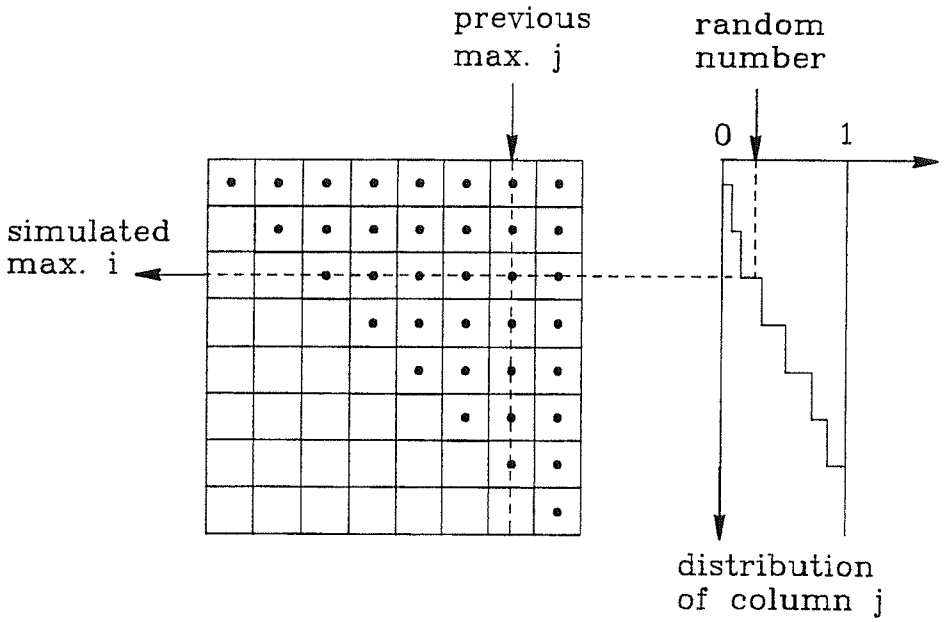

Fig. 2.8 Principle in variable amplitude load simulation.

2.6.2 Determination of the Markov Matrix

For a specific investigation, the ideal way of determining the Markov matrix, is to carry out measurements on location. For general test purposes, however, this is not suitable. The matrix must be determined from assumptions on the stochastic process.

A stationary gaussian stochastic process is fully described by its covariance matrix. From the covariance matrix (alternatively the spectral density function), and its first four

derivatives, it is possible by time integrations to obtain the joint density function of two consecutive extremes $a^{\ell-1}$, a^{ℓ}, $f(a^{\ell-1}, a^{\ell})$, Gluver, [16], and by this, the conditional density function $f(a^{\ell} \mid a^{\ell-1})$. Different matrices are thus obtainable on the basis of different spectral density functions.

2.6.3 Spectral Description

In the investigation carried out at the Department of Structural Engineering of the Technical University of Denmark on welded plate test specimens, three different spectra in 64 x 64 resolution have been applied. The spectra are denoted BROAD64, PMMOD64, and NARROW64. The elements in the matrix have been determined numerically from the spectral density function of the wave elevation spectrum, [16,20]. BROAD64 was evaluated from a truncated white noise spectral density function, NARROW64 from a band limited block spectrum, and PMMOD64 from a modified Pierson-Moscowitz (PM) wave elevation spectrum. The main characteristics of these three spectra are given in Table 2.6. The Root Mean Square - (RMS-) and Root Mean Cube - (RMC-) values given in Table 2.6 correspond to a maximum load level equal to the number of load levels, i.e. 64. The irregularity factor, I, is defined as the number of positive-going mean-value crossings divided by the number of maxima of the stress history. For narrow band loading, the irregularity factor will be close to unity. Typical load histories for fixed offshore structures will be more broad banded, with irregularity factors in the range from $\sim$ 0.6 to 0.8.

Spectrum	BROAD64	PMMOD64	NARROW64
Number of load levels	64	64	64
Irregularity factor, I	0.745	0.817	0.987
Minimum load range	1	1	1
Maximum load range	63	63	63
RMS (rainflow count)	18.6	19.8	22.9
RMC (rainflow count)	21.5	22.6	25.2

Table 2.6 Characteristics of load spectra used in the investigation.

Furthermore, initial test series were carried out using a spectrum, PM32 - a non-gaussian distribution with 32 x 32 resolution - with similar characteristics as PMMOD64, but with more large cycles resulting in a RMC-value that would be equal to 30.1 with 64 load levels

in the spectrum, and with a slightly higher irregularity factor (I = 0.84) than PMMOD64.

Evaluation of the Markov matrix involves numerical determination of the first four spectral moments. Since the PM-spectrum has a tail behaviour of ω^{-5} (where ω is the angular frequency), the fourth order moment is infinite, for which reason a modification is necessary.

Only the PM-spectrum is described in detail, but similar investigations have been carried out for the two other spectra. The spectral density of the modified PM-spectrum is

$$S_{PM}(\omega) = \frac{4}{\pi}\sigma^2\left[\frac{2\pi}{T_z}\right]^4 \omega^{-5}\exp\left\{-\frac{1}{\pi}\left[\frac{2\pi}{T_z}\right]^4 \omega^{-4}\right\} \cdot k(\omega) \tag{2.2}$$

where σ is the standard deviation of the process, and T_z is the zero upcrossing period. The factor $k(\omega)$ is the modification factor, chosen to

$$k(\omega) = \exp\left\{-\left(\frac{\omega}{\omega_t}\right)^8\right\} \tag{2.3}$$

This modification factor will give a relatively sharp but continuous cut off at the angular truncation frequency ω_t, which was chosen to 3 times the peak frequency of the spectrum. This reduction in the low amplitude high frequency content is not considered to be of any importance in the fatigue damage accumulation.

For the test series on the tubular joints, two load spectra - PMMOD32 and PM32 - have been used, both based on the Pierson-Moscowitz wave elevation spectrum. These spectra have an irregularity factor of I = 0.82-0.84.

In Refs. 18 and 27 are given for each of the various spectra used in these investigations the spectral density function, the density of simulated maxima, the density of the rainflow counted stress ranges, an exceedance diagram, and a damage diagram.

Fig. 2.9 shows a comparison between the density of maxima for the three spectra BROAD64, PMMOD64, and NARROW64. Fig. 2.10 shows an example of a simulated load history with 450 extremes, generated by use of the matrix PMMOD64. Examples of typical load histories for the spectra BROAD64, NARROW64 and PM32 may be found in Refs. 18 and 29.

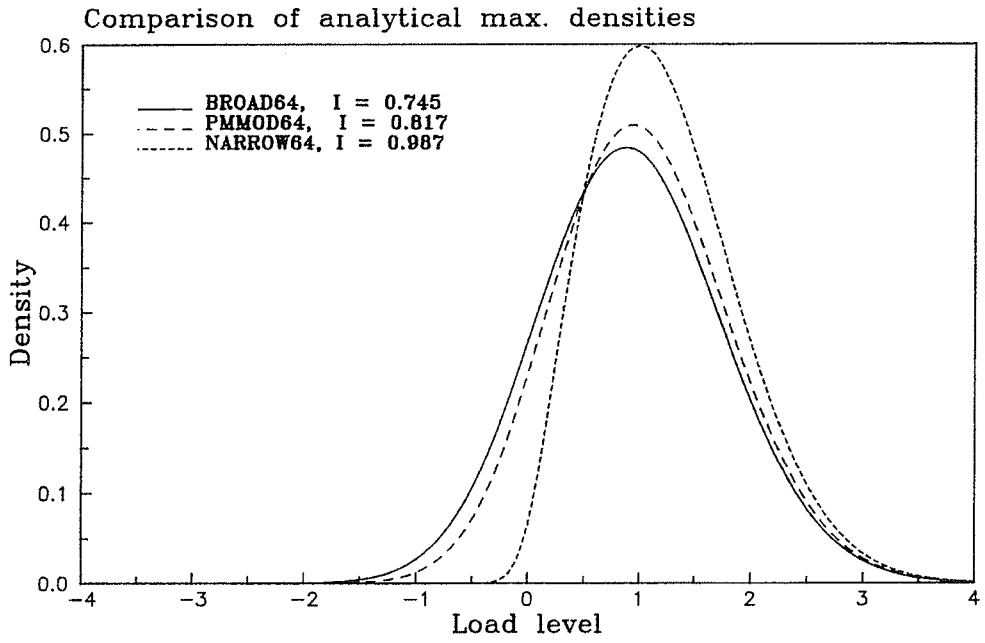

Fig. 2.9 Comparison between densities of maxima for the spectra BROAD64, PMMOD64, and NARROW64.

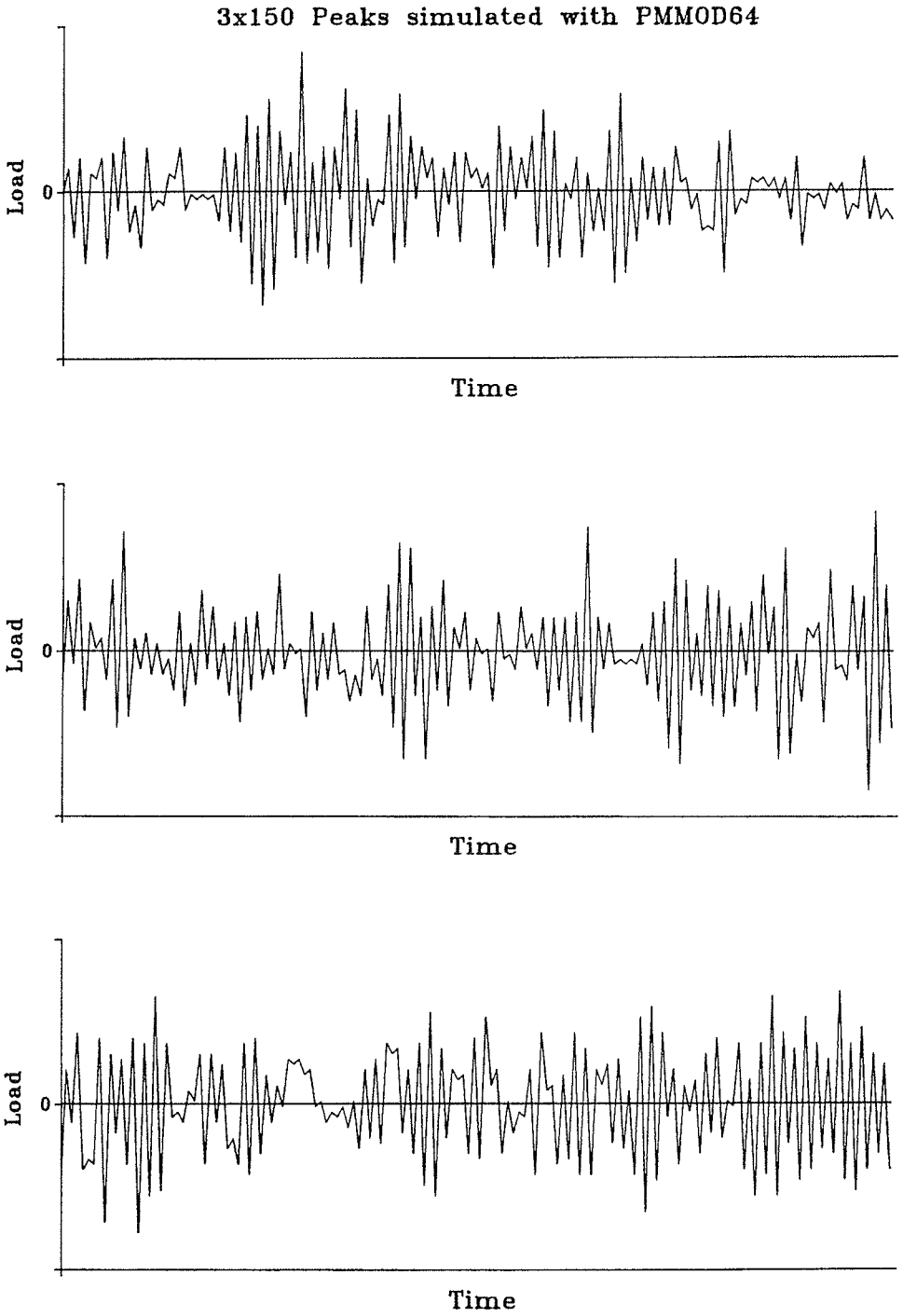

Fig. 2.10 Example of load history. 450 extremes generated by use of PMMOD64.

2.6.4 Equivalent Stress Range and Truncation

Determination of an equivalent stress range in a non-narrowbanded stress history requires more sophisticated cycle counting procedures than for instance peak - to - peak counting. During the stochastic load tests, peak sequences of between 5000 and 20000 cycles are filed. From this file, an equivalent stress range is determined by use of the rainflow counting method. All cycles are registered during the test, but to avoid cycles with stress ranges below the fatigue threshold level, the range distribution from the rainflow counting is truncated, before the equivalent stress range is calculated. No lower truncation to avoid cycles below the fatigue threshold level has been introduced in the load generation algorithm.

The maximum stress range is divided into 128 intervals of equal length, and in each interval (represented by $\Delta\sigma_i$), the number of cycles n_i is counted. With the total number of cycles to failure, $N = \sum_{i=1}^{128} n_i$, the equivalent stress range is calculated from the following equation:

$$\Delta\sigma_e = \left[\frac{\sum_{i=1}^{128} \left(n_i \Delta\sigma_i^m \right)}{N} \right]^{\frac{1}{m}} \tag{2.4}$$

In Eq. 2.4, m is the exponent of the S-N curve, obtained from the corresponding constant amplitude fatigue test series. If the truncation is calculated to take place at a limit between two intervals $\Delta\sigma_{k-1}$ and $\Delta\sigma_k$, the equivalent stress range is calculated from

$$\Delta\sigma_{e,\,trunc} = \left[\frac{\sum_{i=k}^{128} \left(n_i \Delta\sigma_i^m \right)}{\sum_{i=k}^{128} n_i} \right]^{\frac{1}{m}} \tag{2.5}$$

If the truncation is calculated to take place in an interval, the interval is split in two by linear interpolation, and again Eq. 2.5 is used.

This truncation is especially important in the tests on the tubular joints. Here, the ramping between consecutive extremes introduces a very small cycle for almost each step in the ramp, because of the relatively low frequency.

The points that have been plotted in the S-N diagrams correspond to $(\sum_{i=k}^{128} n_i,\ \Delta\sigma_{e,trunc})$.

The actual stress range under which no fatigue crack propagation takes place, $\Delta\sigma_{th}$, has been calculated by use of linear elastic fracture mechanics for each type of test specimen.

The threshold value of the stress intensity factor range, ΔK_{th}, below which no crack growth will occur, can be written as, [14]:

$$\Delta K_{th} = F_S \cdot F_E \cdot F_G \cdot F_T \cdot F_W \cdot \Delta\sigma_{th} \cdot \sqrt{\pi a} \tag{2.6}$$

The correction factors account for:

F_S: Free surface
F_E: Crack shape
F_G: Stress concentrations due to geometrical discontinuity
F_T: Finite plate thickness
F_W: Finite plate width

By assuming a semi-elliptical surface crack with half-axis a (crack depth) and b (b = 2a), the correction factors may be written as:

$$F_S = 1.12 - 0.12 \cdot \frac{a}{b} = 1.06 \tag{2.7}$$

$$F_E = \left\{ 1 + 4.5945 \cdot \left[\frac{a}{2b}\right]^{1.65} \right\}^{-\frac{1}{2}} = 0.8258 \tag{2.8}$$

$$F_T = \sqrt{\sec\left[\frac{\pi a}{2t}\right]} \tag{2.9}$$

$$F_W = 1 \tag{2.10}$$

The geometry correction factor, F_G, is a non-simple function of a. F_G has for the test specimens of the present investigation been determined numerically by FEM calculations. The threshold value of the stress intensity factor range, ΔK_{th}, may be taken as 2.5 MPa $\sqrt{m}$, according to [34, 35]. On this basis, threshold values of the stress range can be found as a function of the crack depth, see Table 2.7.

Crack depth	a = 0.1 mm	a = 3 mm	a = 8 mm
Small plate specimens	80 MPa	27 MPa	-
Large plate specimens	70 MPa	27 MPa	15 MPa

Table 2.7 Threshold stress range at selected crack depths for plate test specimens.

On the basis of these values, the truncation levels have been chosen as:

Small plate specimens: $\Delta\sigma_{th} = 25$ MPa

Large plate specimens: $\Delta\sigma_{th} = 15$ MPa

The tubular joint test specimens will have the same $\Delta\sigma_{th}$ as the large plate specimens, but here the measured stresses are extrapolated to calculate the hot spot stress, $\Delta\sigma_{HS}$, which is the stress to be truncated. For this reason, $\Delta\sigma_{th}$ on the measured stresses is chosen as 10 MPa instead of 15 MPa.

It should be emphasized that this method is an approximate method because of the uncertainties in ΔK_{th} and the empirical correction factors in the expression for ΔK. Nevertheless, it is appropriate, since $\Delta\sigma_e$ is unsensitive to the truncation level, as demonstrated in Fig. 2.11. Furthermore, it may be seen from this figure that a change in truncation level will only move the point in the S-N diagram along a curve with $m \sim 3$, i.e. practically the same S-N regression line will be the result.

The Markov matrices used in the present investigation have been determined with an upper truncation level at 4 times the standard deviation of the process. This corresponds to neglecting the highest 0.03% of the total probability.

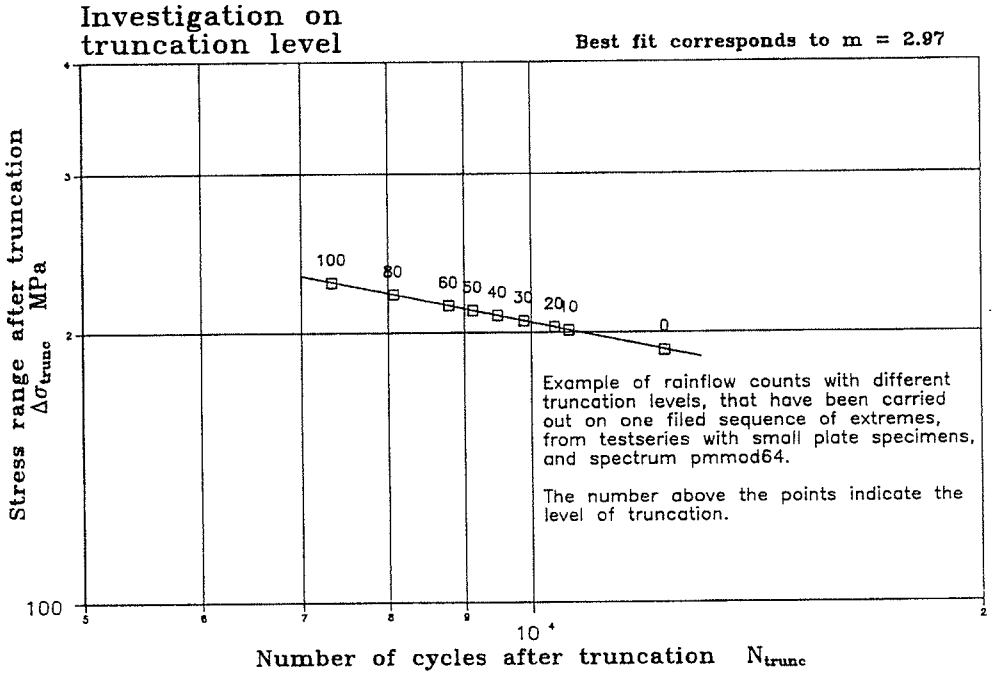

Fig. 2.11 Consequence of chosen truncation level illustrated by an example. A change in truncation level moves the point along a curve with m $\sim$ 3.

3. STATIC TEST RESULTS

Before and during the fatigue tests on the tubular joint test specimens, static tests were carried out. One of the purposes of the static tests was to measure the concentrated rotation in the joint due to local plate bending, i.e., the joint flexibility. This flexibility is of interest in relation to the analysis of the structure, and thus to the fatigue life. Implementation of flexible joints in finite element analysis of offshore structures indicates clear reductions of the bending moments in the branches, resulting in increases in the fatigue life of the structure, compared with a rigid joint analysis.

Another purpose of the static tests was to determine the local bending stresses in the chord wall. These stresses were obtained from strain gages placed on both the outer side and the inner side of the chord wall. These stress distributions are used as a basis for a fracture mechanics determination of the fatigue life, see Ref. 34. The strain gage measurements have shown that a high percentage of the stresses - up to 70-80% - in the hot-spot areas is due to local plate bending.

The tubular joints were instrumented to determine hot spot stresses at the weld toe and to give sufficient information of the total stress distribution in the most interesting areas to compare measurements and results of finite element analysis. Furthermore, the dependence of the stresses and joint stiffness on the crack propagation was investigated.

The static tests were carried out at load levels, which gave a hot spot stress range that was approximately 40% higher than the equivalent stress range in the tests with stochastic loading.

In connection with the project, a finite element (FEM) analysis was carried out to determine stresses and deformations in the tubular joint test specimens. Isotropic shell elements with eight nodes were used in this analysis. The welds were modelled by use of brick elements. Linear elasticity of the material was assumed in the analysis. The main results obtained in the FEM analysis may be found in Ref. 23.

3.1 Determination of Stresses and Deformations

For the tubular joint test specimens, the hot spot stresses were determined both by use of strain gages and from FEM analysis. In the determination of the experimental values of the hot spot stresses, standard strain gage measuring points were used. The measuring points were defined from the following formulae, [12, 21], giving the distances from the weld toe.

For both chord and branch:

$$a = 0.2 \cdot \sqrt{\frac{d_1 \, t_1}{2}} = 8 \text{ mm} \tag{3.1}$$

For the chord:

$$b = 0.4 \cdot \sqrt[4]{\frac{d_1 \, t_1 \, d_0 \, t_0}{4}} = 21 \text{ mm} \tag{3.2}$$

and for the branch:

$$b = 0.65 \cdot \sqrt{\frac{d_1 \, t_1}{2}} = 26 \text{ mm} \tag{3.3}$$

In these formulae,

d_0 = the diameter of the chord
d_1 = the diameter of the branch
t_0 = the wall thickness of the chord
t_1 = the wall thickness of the branch

The standard strain gage instrumentation in the tests consists of 24 xy-gages (axial and tangential strains), i.e. a total of 48 strain gages, placed as shown in Fig. 3.1. Furthermore, one of the tubular joint test specimens in conventional offshore structural steel was instrumented with strain gages at several other locations to make possible a comparison between results obtained in the finite element analysis and experimental results.

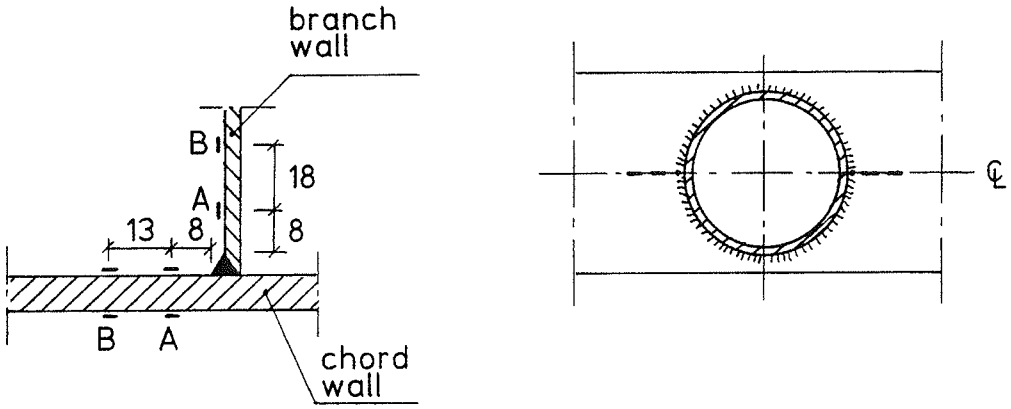

Fig. 3.1 Strain gage instrumentation of tubular joint test specimens.

The displacements were in the first series of tests on the tubular joints measured at 10 points, as shown in Fig. 3.2. The displacement measurements were primarily taken for a comparison with the results obtained in the FEM analysis, but furthermore the two horizontal displacements, measured at the top of the branches, form the basis for a calculation of the concentrated rotation in the joint due to local plate bending, i.e. the joint flexibility, see Ref. 27.

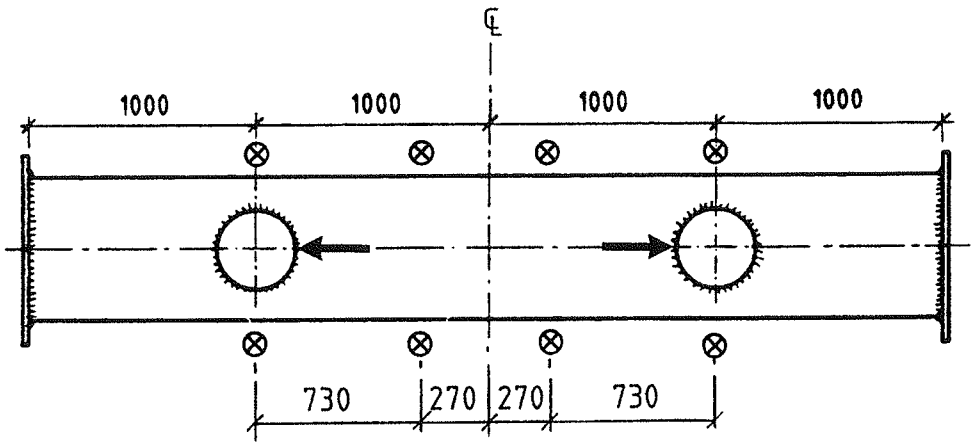

Fig. 3.2 Measuring points for displacement measurements.

3.2 Measured Stresses

The most important stresses with respect to fatigue are the stresses in the hot spot region. The actual hot spot stresses have been calculated for each of the static tests. The measured hot spot stress, as given in Table 3.1, is defined as the axial stress at the weld toe obtained by linear extrapolation of the axial stresses in points A and B, see Fig. 3.1. Test No. W3 was carried out by T. Vejrum and J.A. Nielsen as a part of their M.Sc. project, and details of the results from test No. W3 may be found in Ref. 33.

The experimental hot spot stresses are compared with the empirical stresses obtained by using current offshore code formulae, [12], and with the stresses obtained from the FEM analysis, using 2-dimensional shell elements, [23]. This comparison is given in Table 3.1.

The hot spot stresses given in Table 3.1 have been determined from the longitudinal strain gages in the symmetry plane of the test specimen, i.e. the stresses are axial hot spot stresses.

	CHORD				BRANCH			
	Towards the end		Towards the centre		Towards the end		Towards the centre	
	+30kN	-30kN	+30kN	-30kN	+30kN	-30kN	+30kN	-30kN
Test No. W1	85 83	- 86 - 82	- 95 -103	95 103	69 73	- 69 - 72	- 70 - 65	72 67
Test No. W2	87 81	- 86 - 80	- 92 - 85	92 85	71 69	- 70 - 69	- 71 - 68	70 68
Test No. W3	87 82	- 87 - 81	- 89 - 93	88 92	64 67	- 63 - 66	- 62 - 75	62 75
Mean value of experimental results	84	- 84	- 93	93	69	- 68	- 69	69
FEM analysis, [23]	88	- 88	-101	101	47	- 47	- 52	52
Design code, [12]	126	-126	-126	126	107	-107	-107	107

Table 3.1 Comparison of axial hot spot stresses at a load of P = ± 30 kN. Stresses in MPa.

The rather large scatter is primarily due to differences in the local weld geometry. Furthermore, inevitable inaccuracies in the placing of the strain gages will have some effect.

In all of the tests on the tubular joints in high-strength steel, the fatigue cracks developed at the edge of the weld and propagated into the main tube wall until final fatigue failure in the main tube.

It appears from Table 3.1 that for the hot spot stresses in the chord, a good agreement is obtained between the experimental results and the results of the finite element analysis. The code formula gives stresses in the chord that are 25-50% higher than the test and finite element results. Table 3.1 further shows that the hot spot stresses in the branch are somewhat lower than in the chord.

Also the changes in the hot spot stresses with the fatigue crack propagation have been studied. In Figs. 3.3, 3.4, and 3.5, the development of the fatigue cracks and the stresses in the chord wall are shown. The results in these figures are from measurements in tests No. W1 and W2.

From Figs. 3.3-3.5 it may be seen that the stresses at the crown in this case are practically unaffected by the cracks, until these become quite long. When the crack propagation has reached a stage where a crack is present in front of the measuring points at the crown, the stresses decrease rapidly as the crack propagates through the chord wall.

In the tests carried out, the fatigue cracks in most cases initiated some distance from the crown, as may be seen in Fig. 3.3. This behaviour was also to be expected with background in the results obtained in the FEM analysis, which showed a maximum in von Mises stresses at an angle of about 30^{o} from the crown. However, in other cases, the crack development was found to initiate at the crown or close to the crown, and the crack then propagated from here.

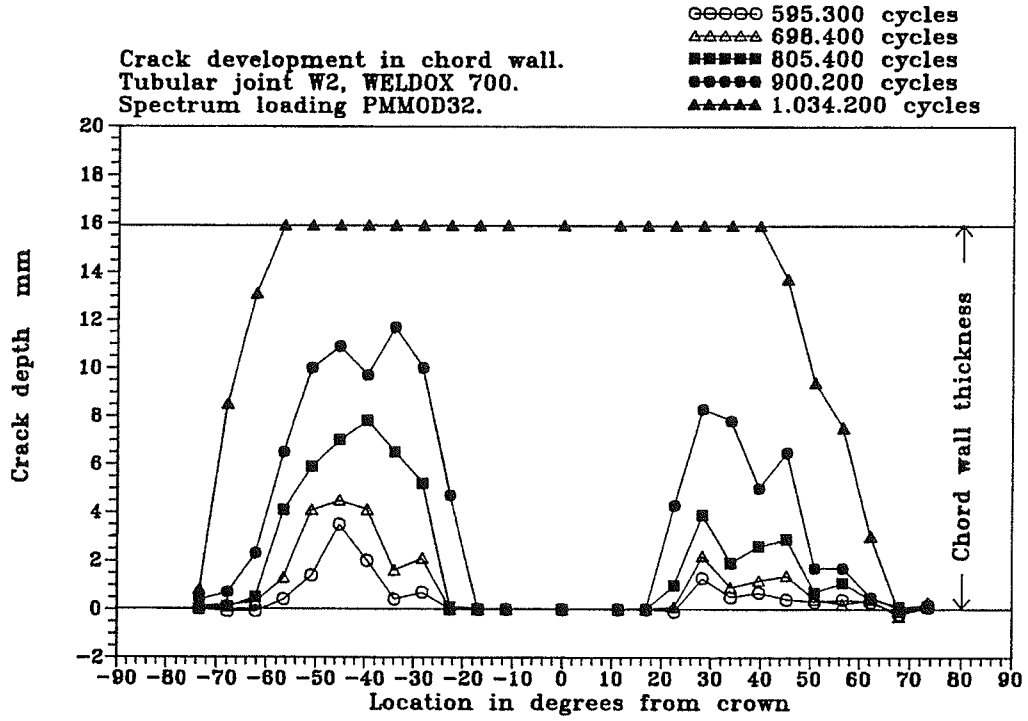

Fig. 3.3 Crack depth development during fatigue test. Test No. W2.

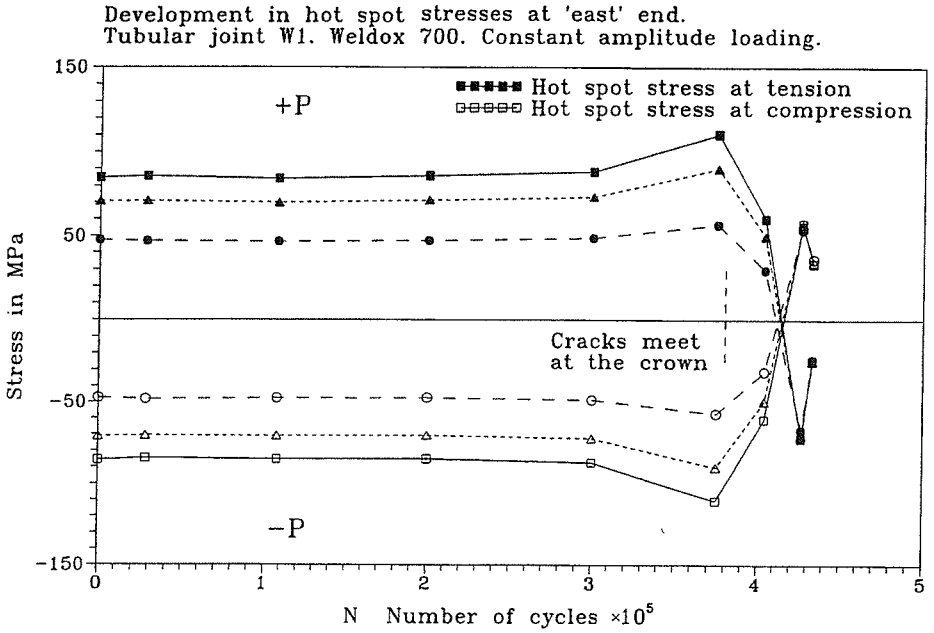

Fig. 3.4 Stress development on the outer side of the chord wall. Test No. W1. "East" end of test specimen.

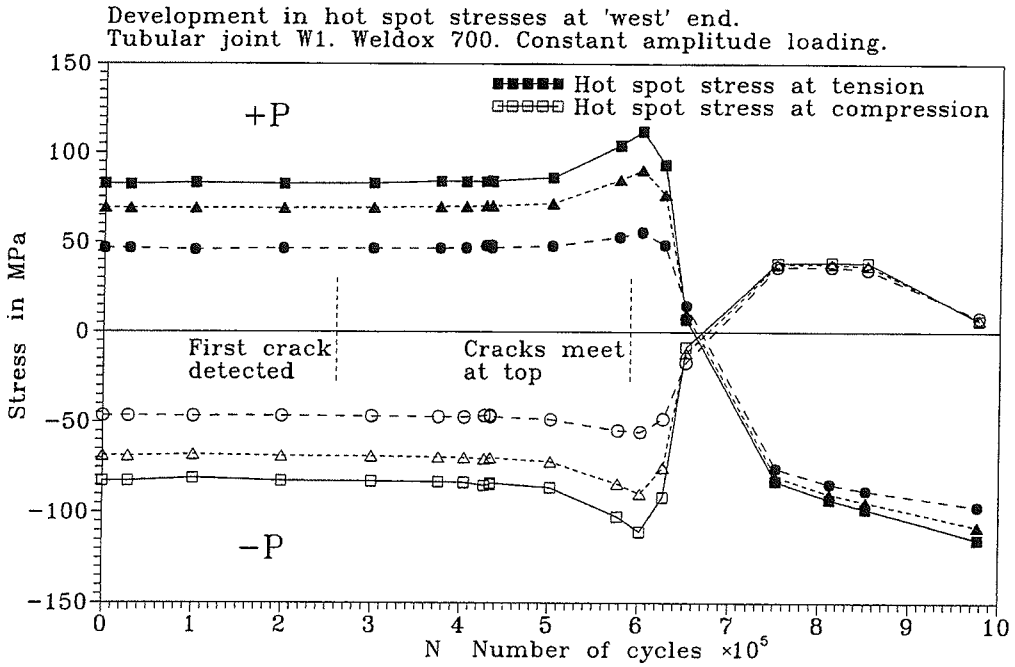

Fig. 3.5 Stress development on the outer side of the chord wall. Test No. W1. "West" end of test specimen.

The stress and strain distributions in the symmetry plane of the tubular joint test specimens were determined from both strain gage measurements and FEM analysis. Examples of stress and strain distributions may be found in Ref. 27.

3.3 Rotational Stiffness of Tubular Joints

In test No. W1, the displacements of the branches were measured to determine the initial joint stiffness and the effect of the crack development on the stiffness of the joint during the test.

The mean value of the initial joint stiffness for the two joints in the test specimen was $2.67 \cdot 10^7$ Nm/rad. For the tubular joints in conventional offshore structural steel with a similar geometry, an initial stiffness of $2.66 \cdot 10^7$ Nm/rad was found.

The test showed that when the fatigue cracks propagated across the crown, the joint stiffness decreased rapidly. The joint stiffness measured at the time, when fatigue failure occurred, was reduced to about half the value of the initial joint stiffness.

At the "east" end of the test specimen, cracks developed across the crown at about 350000 cycles, and the joint stiffness decreased rapidly shortly after. Cracks developed across the crown at the "west" end after about 600000 cycles. For the "east" connection, cracks developed mainly on one side of the branch (the side towards the end), while for the "west" connection, continuous cracks could be observed on both sides of the secondary tube.

3.4 Comparison of Test Results with Usual Design Procedures

The fatigue life of tubular joints is normally determined by use of the empirical stress concentration factor method. Based on a large number of experiments and numerical simulations, formulae have been determined, from which the hot spot stresses can be estimated.

The expressions cover geometrically plane joints, taking into account the load type, the joint geometry, and the configuration of the branches. The local weld geometry is not taken into account. The stress concentration factor, SCF, is defined from the following equation:

$$\sigma_{\text{hot spot}} = \text{SCF} \cdot \sigma_{\text{nominal}} \tag{3.4}$$

where the hot spot stress, $\sigma_{\text{hot spot}}$, is the maximum stress at the weld toe, excepting very local stress concentrations due to notch effects from the weld toe. The stress, σ_{nominal}, is the maximum nominal stress from bending moment and/or normal force in the cross section, a-a, shown in Fig. 3.6.

The stress concentration factors that were obtained from the strain gage measurements for the tubular joints No. W1 and W2 are given in Table 3.2. Similar results for the tubular joint No. W3 may be found in Ref. 33.

The SCF-value is about 1.7 for the branch, regardless of the position. For the chord, there is a tendency - as expected - that the SCF-value is larger towards the centre (2.1-2.4) than towards the end ($\sim$ 2.0).

For the tubular joint No. W1, fatigue failure did not occur at the positions in the chord with the largest SCF-values, even though the stress concentration was about 20% higher at these

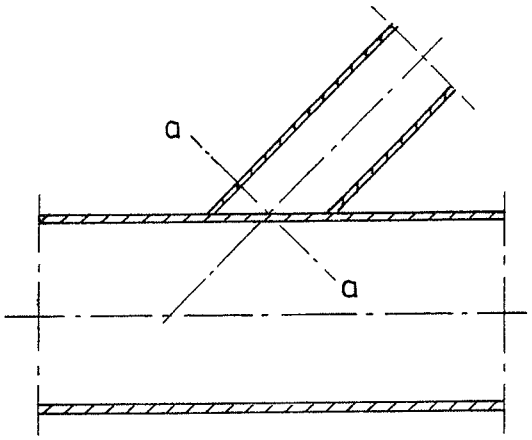

Fig. 3.6 Cross section for determination of $\sigma_{nominal}$.

positions.

For all the tubular joints tested in the present investigation, values of the stress concentration factors, determined both from the static tests and from empirical formulae, [12], are given in Table 3.3. For a comparison, Table 3.3 also gives the SCF-values that were obtained in the similar investigation on tubular joints in conventional offshore structural steel, [18].

Test specimen	Tube	Position	SCF
W1	Chord	Towards the end	2.04*)
		Towards the centre	2.41
	Branch	Towards the end	1.73
		Towards the centre	1.66
W2	Chord	Towards the end	2.03
		Towards the centre	2.14*)
	Branch	Towards the end	1.69
		Towards the centre	1.68

Table 3.2 Stress concentration factors obtained in tests No. W1 and W2. *) Final fatigue failure occurred at these positions.

It is assumed that the main reasons for the differences that may be observed in Table 3.3, between the SCF-values from the design code, [12], and the experimental values, are that the largest hot spot stresses will not occur at the measuring points at the crown, and the empirical formulae may in general be expected to be conservative.

	JOINTS IN CONVENTIONAL OFFSHORE STRUCT. STEEL				JOINTS IN HIGH-STRENGTH STEEL			
	CHORD		BRANCH		CHORD		BRANCH	
	End	Centre	End	Centre	End	Centre	End	Centre
Design code, [12]	2.93	2.93	2.56	2.56	3.06	3.06	2.59	2.59
Mean value of experimental results	1.96	2.18	1.89	1.86	2.04	2.26	1.67	1.67

Table 3.3 Stress concentration factors obtained from empirical formulae and from static tests.

4. FATIGUE TEST RESULTS

In the following are given the results that have been obtained in the test series on the tubular joints. For the plate test specimens, the characteristics - plate thicknesses, types of welds, materials, etc. - were chosen to correspond as much as possible to the tubular joints, and also the variable amplitude loading used in both investigations was identical. For a comparison with the tubular joint test results, the main results obtained in the test series on the plate test specimens are also included. Details of the results that were obtained in the investigation on the plate test specimens may be found in Ref. 29.

For both types of test specimens, initial test series with constant amplitude loading were carried out as a reference, and also - for the plate test specimens - to obtain the actual value of the exponent m for calculation of the equivalent stress ranges of the tests with variable amplitude loading, cf. Eq. 4.1. In the test series with variable amplitude loading, the different load spectra described previously have been used. Table 4.1 gives the number of tests that has been carried out in each test series with test specimens in high-strength steel.

In the results from the variable amplitude tests, the stress parameter used is the equivalent constant amplitude stress range, $\Delta\sigma_e$, defined as

$$\Delta\sigma_e = \left[\frac{\sum_i (n_i \cdot \Delta\sigma_i^m)}{N} \right]^{1/m} \qquad (4.1)$$

in which

n_i = number of cycles of stress range $\Delta\sigma_i$

$\Delta\sigma_i$ = variable amplitude stress range

Test series	Constant amplitude	Spectrum: BROAD64	Spectrum: PMMOD32 or PMMOD64
Small plate specimens	18	21	21
Large plate specimens	13	12	10
Tubular joints	2	-	4

Table 4.1 Number of completed fatigue tests in each test series.

N = total number of cycles ($= \Sigma_i n_i$)

m = slope of corresponding constant amplitude S-N line

4.1 Test Series on Welded Plate Specimens

For the test results obtained in each test series on the plate specimens, the data are fitted to an expression

$$\log N = \log A - m \cdot \log \Delta\sigma \tag{4.2}$$

by the method of least squares. In Eq. 4.2, m and A are constants, N is the number of cycles to failure, and $\Delta\sigma$ is the stress range.

Examples of the results that have been obtained in the test series on the plate specimens are shown in the S-N diagrams in Figs. 4.1-4.2. These figures show the results of the test series with the spectrum BROAD64, together with the results obtained in the corresponding constant amplitude test series. In the S-N diagrams, points marked with an arrow correspond to a test with a non-broken test specimen. For a comparison, all the S-N lines that have been obtained in these test series are shown in Fig. 4.3 for the small plate specimens, and in Fig. 4.4 for the large plate specimens. The main data for these S-N lines are summarized in Table 4.2.

Test series	log A	m	Correlation coefficient, ρ
Constant amplitude, small plate specimens	12.962	2.935	-0.84
Constant amplitude, large plate specimens	12.066	2.741	-0.98
Spectrum: BROAD64, small plate specimens	12.511	2.862	-0.85
Spectrum: BROAD64, large plate specimens	11.724	2.670	-0.99
Spectrum: PMMOD64, small plate specimens	12.416	2.791	-0.73
Spectrum: PMMOD64, large plate specimens	10.739	2.204	-0.98

Table 4.2 Summary of results obtained in test series on welded plate specimens.

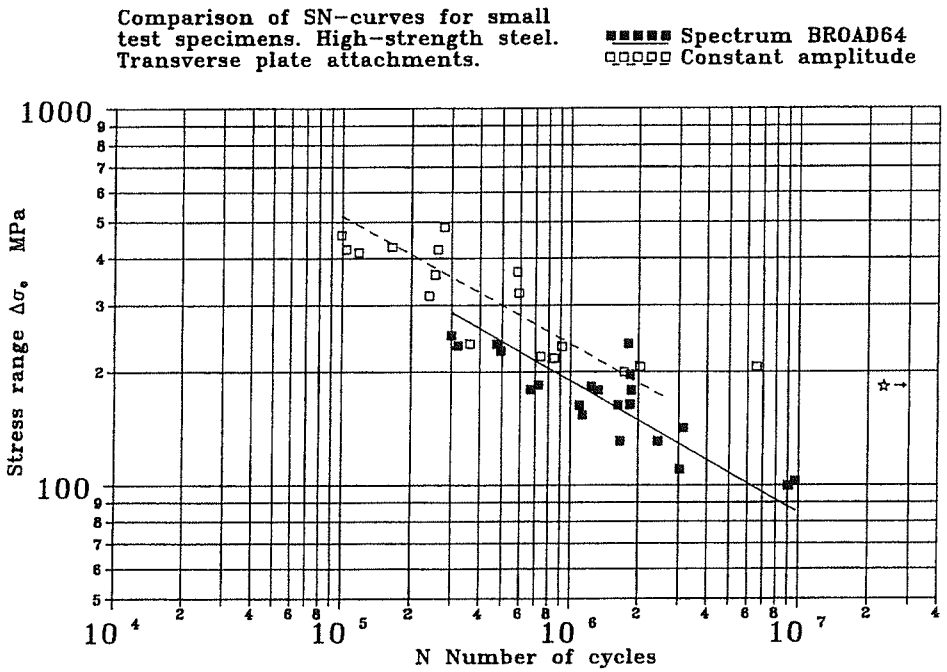

Fig. 4.1 Results obtained from variable amplitude tests with BROAD64 spectrum and constant amplitude tests. Small plate specimens with transverse attachments.

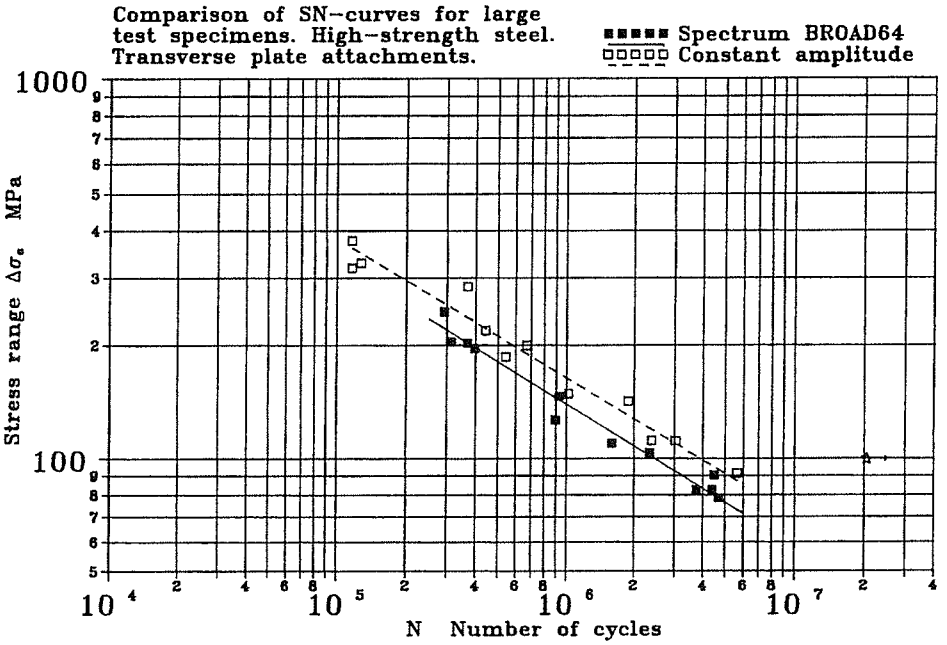

Fig. 4.2 Results obtained from variable amplitude tests with BROAD64 spectrum and constant amplitude tests. Large plate specimens with transverse attachments.

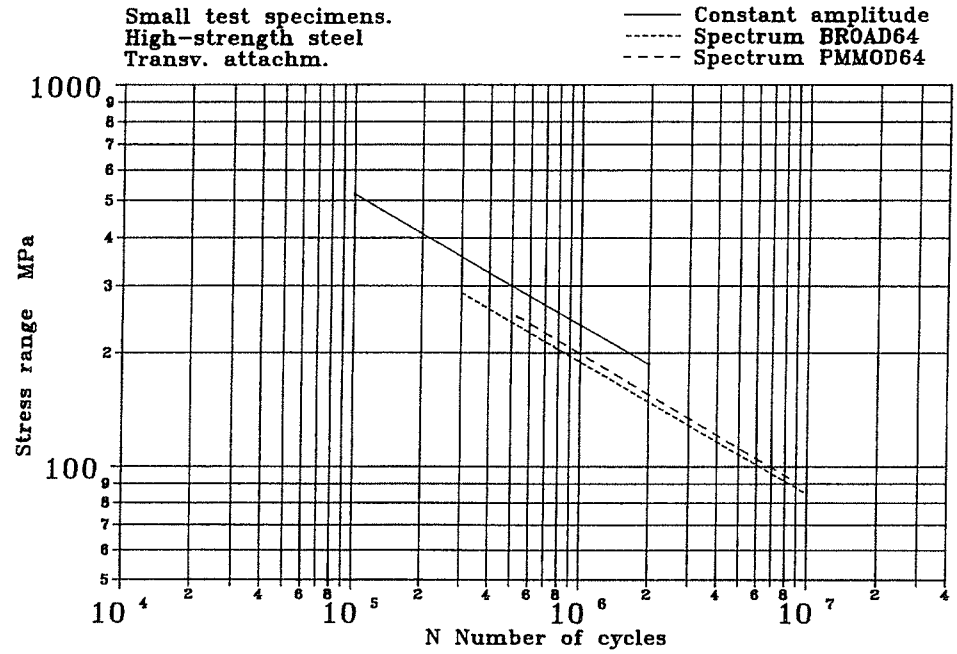

Fig. 4.3 Linear regression S-N lines from test series on small plate specimens with transverse attachments.

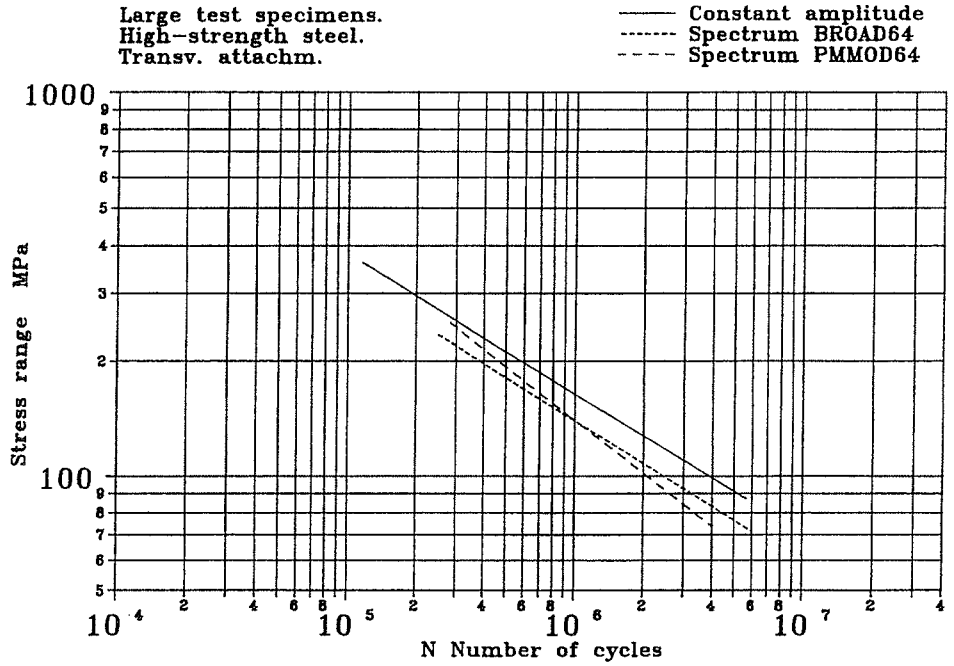

Fig. 4.4 Linear regression S-N lines from test series on large plate specimens with transverse attachments.

4.2 Test Series on Tubular Joints

The number of tests on the full-scale tubular joints in high-strength steel that has been carried out in the present investigation is insufficient to make possible a statistical treatment of the test data. The results that have been obtained are given in Tables 4.3-4.4 and shown in the S-N diagrams in Figs. 4.5-4.6. For a comparison, the results that were obtained in the similar investigation on tubular joints in conventional offshore structural steel are shown in Figs. 4.7-4.8, [18]. Stress ranges in the variable amplitude tests are equivalent constant amplitude stress ranges, using a value of m = 3. Details of the results obtained in the test on tubular joint No. W3 may be found in Ref. 33. In Figs. 4.5-4.8, points marked with an arrow means no fatigue failure at the corresponding location in the test specimen.

After fatigue failure at one of the test joints, this end of the test specimen was strengthened by use of bracing, as described in section 2.5.2, and the test was continued until fatigue failure also occurred at the other joint. Each test thus provides 4 points in each of the S-N diagrams given in Figs. 4.5-4.8.

Test No.	Type of loading	Side of tube, towards:	Hot spot stress range, $\Delta\sigma_{hot\ spot}$, in MPa	Number of cycles to failure, N x 10^3
W1	Constant amplitude	end	165	434
		centre	187	> 434
		centre	201	> 977
		end	162	977
W2	Spectrum: PMMOD 32	end	117	> 1429
		centre	126	1429
		centre	119	1033
		end	112	> 1033
W3	Spectrum: PMMOD32	end	119	> 1221
		centre	123	1221
		centre	128	1304
		end	112	> 1304

Table 4.3 Results obtained in test series on tubular joints in high-strength steel. Stresses in chord.

Test No.	Type of loading	Side of tube, towards:	Hot spot stress range, $\Delta\sigma_{hot\ spot}$, in MPa	Number of cycles to failure, N x 10^3
W1	Constant amplitude	end centre centre end	134 139 129 144	> 434 > 434 > 977 > 977
W2	Spectrum: PMMOD32	end centre centre end	96 96 96 94	> 1429 > 1429 > 1033 > 1033
W3	Spectrum: PMMOD32	end centre centre end	89 88 103 93	> 1221 > 1221 > 1304 > 1304

Table 4.4 Results obtained in test series on tubular joints in high-strength steel. Stresses in branch.

In all of the tests on the tubular joints in these two series, the fatigue cracks developed at the edge of the weld and propagated into the main tube wall until final fatigue failure in the main tube.

By the manufacturing of the tubular joints, some areas around the weldments were ground to clean the tubes. Some parts of the weld toe were unintentionally ground as well, making the transition from the main tube to the welding smooth and thereby reducing the stress concentration at these points. Especially the welds in tubular joint No. W2 were affected by the grinding, and during the fatigue test on this test specimen, no fatigue crack initiation was observed in these areas, and the crack development was retarded when a fatigue crack propagated along an affected weld toe.

Fig. 4.9 shows a part of the weld between main tube and secondary tube in test No. W2. Some of the areas with grinding may be seen in this photo.

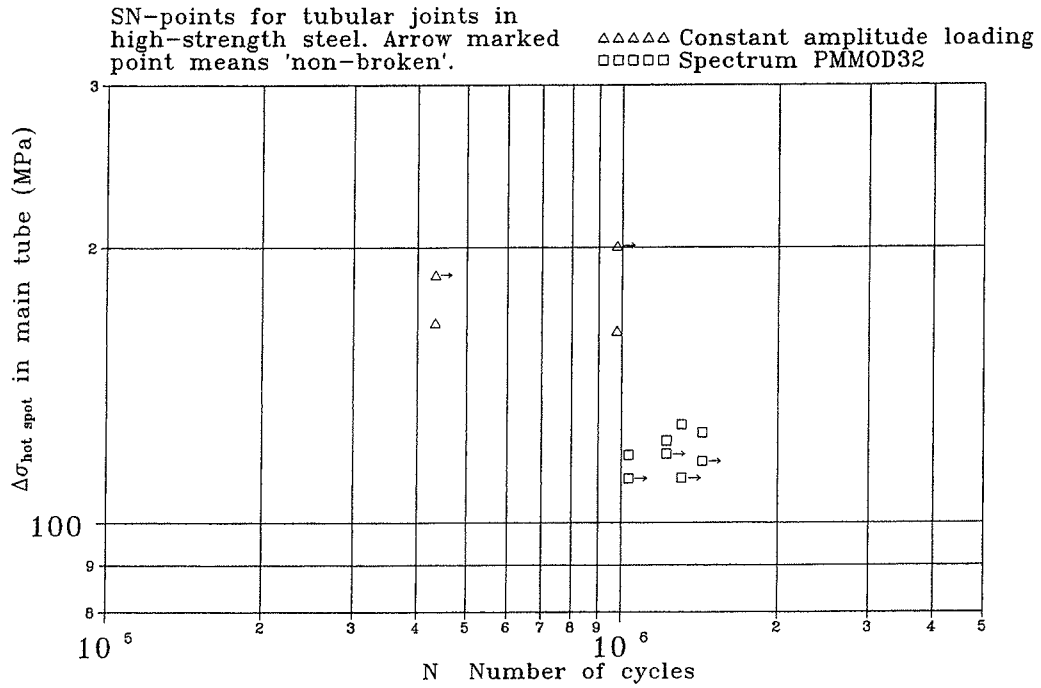

Fig. 4.5 Results obtained in test series on tubular joints in high-strength steel. Stresses in chord.

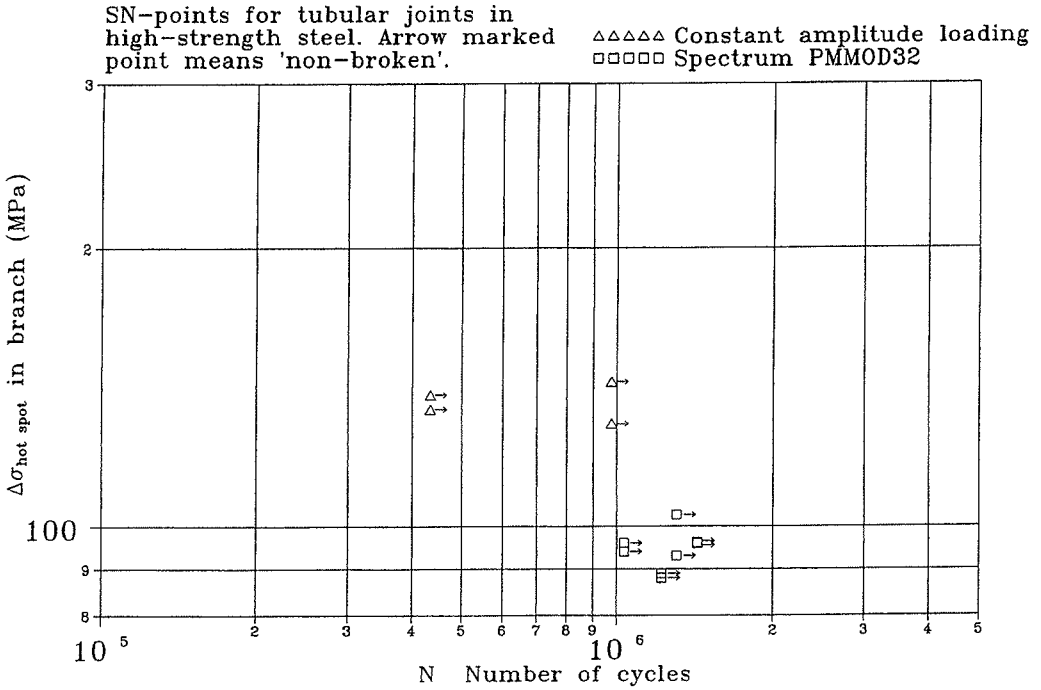

Fig. 4.6 Results obtained in test series on tubular joints in high-strength steel. Stresses in branch.

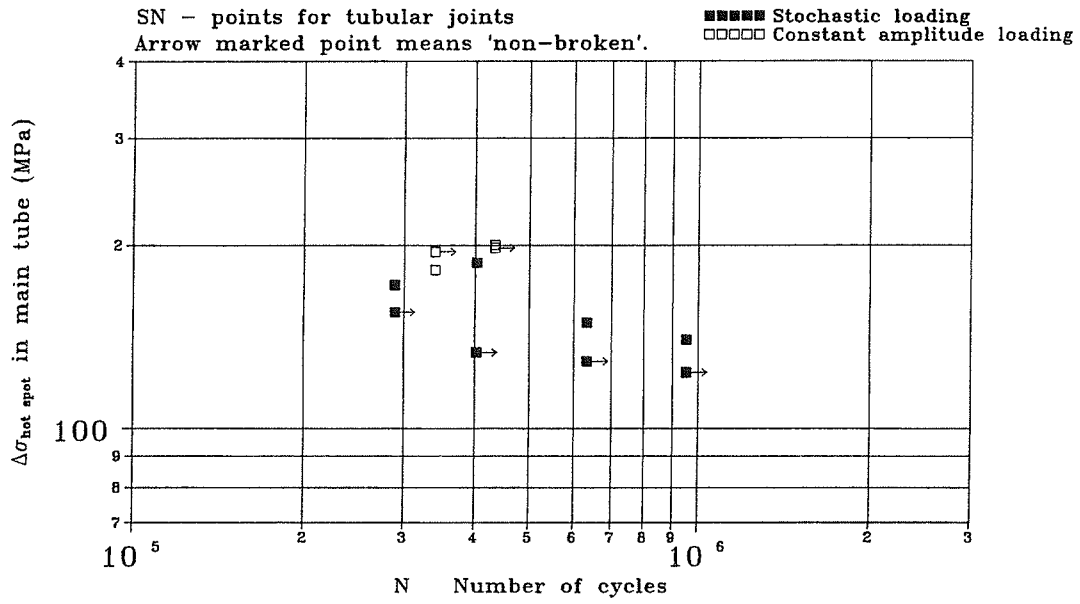

Fig. 4.7 Results obtained in test series on tubular joints in conventional offshore structural steel. Stresses in chord.

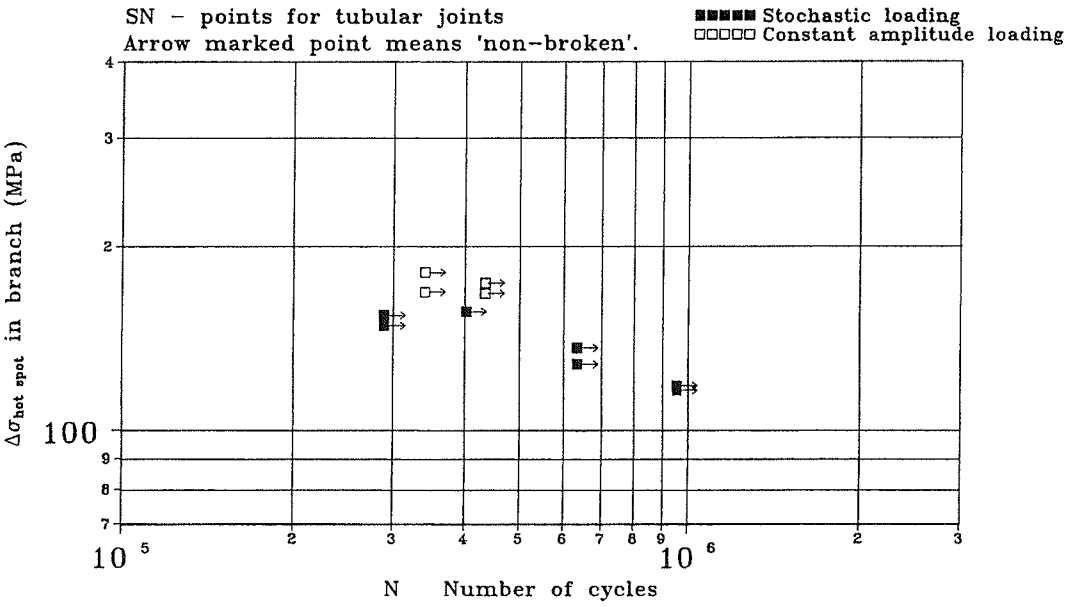

Fig. 4.8 Results obtained in test series on tubular joints in conventional offshore structural steel. Stresses in branch.

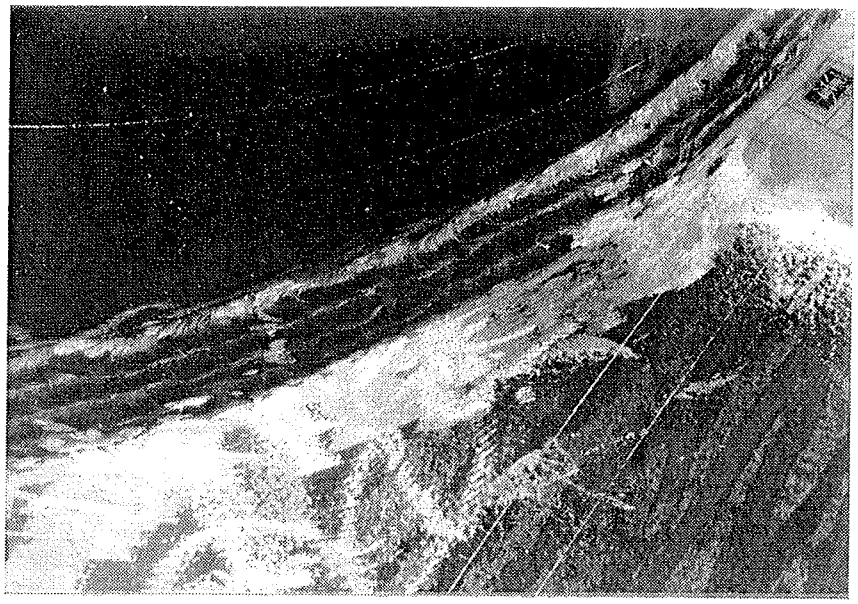

Fig. 4.9 Weld between main tube and secondary tube in test No. W2. Areas with grinding may be seen.

The test results that have been obtained in the test series on the welded plate specimens and the tubular joints make possible comparisons between fatigue lives under constant amplitude loading and under variable amplitude loading, and between joints in high-strength steel and in ordinary offshore structural steel. A discussion of the results obtained is given in the following chapter, Fatigue Test Observations.

4.3 Bending and Membrane Stresses in Tubular Joints

A part of the stresses measured near the crown is caused by local bending. For the tubular joints W1 and W2, the division between local bending stresses and global membrane stresses has been investigated. The expressions used to calculate the two stress components are:

$$\sigma_m = \sigma_{inside} + \frac{\sigma_{outside} - \sigma_{inside}}{2} \tag{4.3}$$

$$\sigma_b = \sigma_{outside} - \sigma_m \tag{4.4}$$

At the measuring points near the weld toe, the local bending stresses are about 70-80% of the

total stresses. At the measuring points further away from the weld toe, the influence of the local bending is reduced, and the bending stresses amount to about 50-60% of the total stresses.

Near the crown, the global membrane stresses are fairly constant, about 16-19 MPa, while the bending stresses near the weld toe are 49-58 MPa, and further away decrease to 25-32 MPa, corresponding to a load of P = 30 kN.

4.4 Measurements of Stresses during Fatigue Tests

During the fatigue tests on the tubular joints, the stresses were registered by the strain gages mounted on the test specimens, and peak value sequences were filed on a computer. In Fig. 4.10, the distribution of rainflow counted stress ranges, for the constant amplitude loading on test specimen W1, is shown.

Some small stress ranges are registered at levels below 5 MPa. These stress ranges represent electrical noise in the system, and minor dynamic responses. The majority of the measured stress ranges has a value of about 135 MPa, and Fig. 4.10 shows that the correct stress range

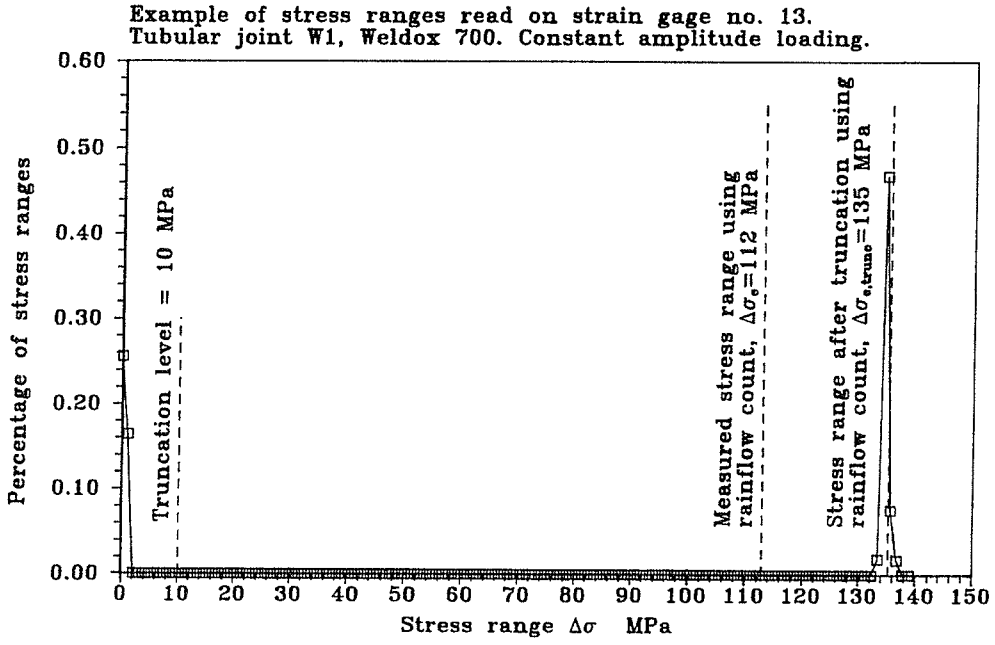

Fig. 4.10 Distribution of rainflow counted stress ranges. Test No. W1.

is found when using rainflow count and a truncation level of 10 MPa on the registered stress peak sequences.

4.5 Fatigue Crack Initiation in Tubular Joints

For all the tubular joints, the initiation of the fatigue cracks that later developed into through-cracks in the chord wall, was studied. Table 4.5 shows for the two tubular joints in each test, the number of cycles to the first detection of fatigue cracks at the joint and the number of cycles to the development of a through-crack in the chord wall.

Test No.	Tubular joint at	Number of cycles to crack detection	Number of cycles to through-crack in chord wall	Crack initiation life as a percentage of total fatigue life, in %
W1	"east" end	260000	433600	60
	"west" end	260000	977000	27
W2	"east" end	410000	1428900	29
	"west" end	410000	1032800	40
W3	"east" end	429000	1220700	35
	"west" end	429000	1304000	33

Table 4.5 Number of cycles to crack initiation and to through-crack in chord wall.

In the present investigation, the crack initiation life is defined as the number of cycles to the detection of the first very small cracks by use of "spot check" spray. When "spot check" is sprayed on an area with fatigue cracks, the pulsating movement will open and close the cracks, and thereby create small bubbles in the fluid. At this stage of the crack development, the cracks cannot be seen without the use of "spot check", and the size of the crack depth is smaller than the accuracy of the AC-potential drop equipment ($\sim$ 0.2 mm).

Test No. W1 was the first test carried out in this investigation, and the use of "spot check" spray had not been perfectioned at this time. Thus, initial cracks may have developed earlier than indicated here in test No. W1.

For details of the results obtained for the tubular joints in test No. W3, see Ref. 33.

It may be seen from Table 4.5 that cracks typically have been detected after about 30-40% of the total fatigue life.

4.6 Fatigue Crack Development in Tubular Joints

The fatigue crack development at the welding between chord and branch was measured using AC-potential drop technique. Furthermore, visual inspections with the use of "spot check" spray were carried out to observe the fatigue crack initiation stages, as described in section 4.5.

As mentioned, the first cracks were typically detected after about 30-40% of the total fatigue life. The cracks consisted of several minor crack spots, situated at points at an angle of about 25-60° from the crown. These cracks continued to grow, and eventually created continuous crack patterns on both sides of the crown. When the cracks developed across the crown, only a small part of the fatigue life was left over, and when the first through-crack was observed, about 5000-40000 cycles remained. In the final stages, the crack gap was about 1-2 mm as indicated in Fig.4.11.

Fig. 4.11 Fatigue crack in chord at edge of weld. Test No. W1.

The cracks do not develop perpendicular into the tubes from the surface, but at an angle of about 70-80° as shown in Fig. 4.12. In two cases, small surface cracks were observed perpendicular to the cracks at the weld toe.

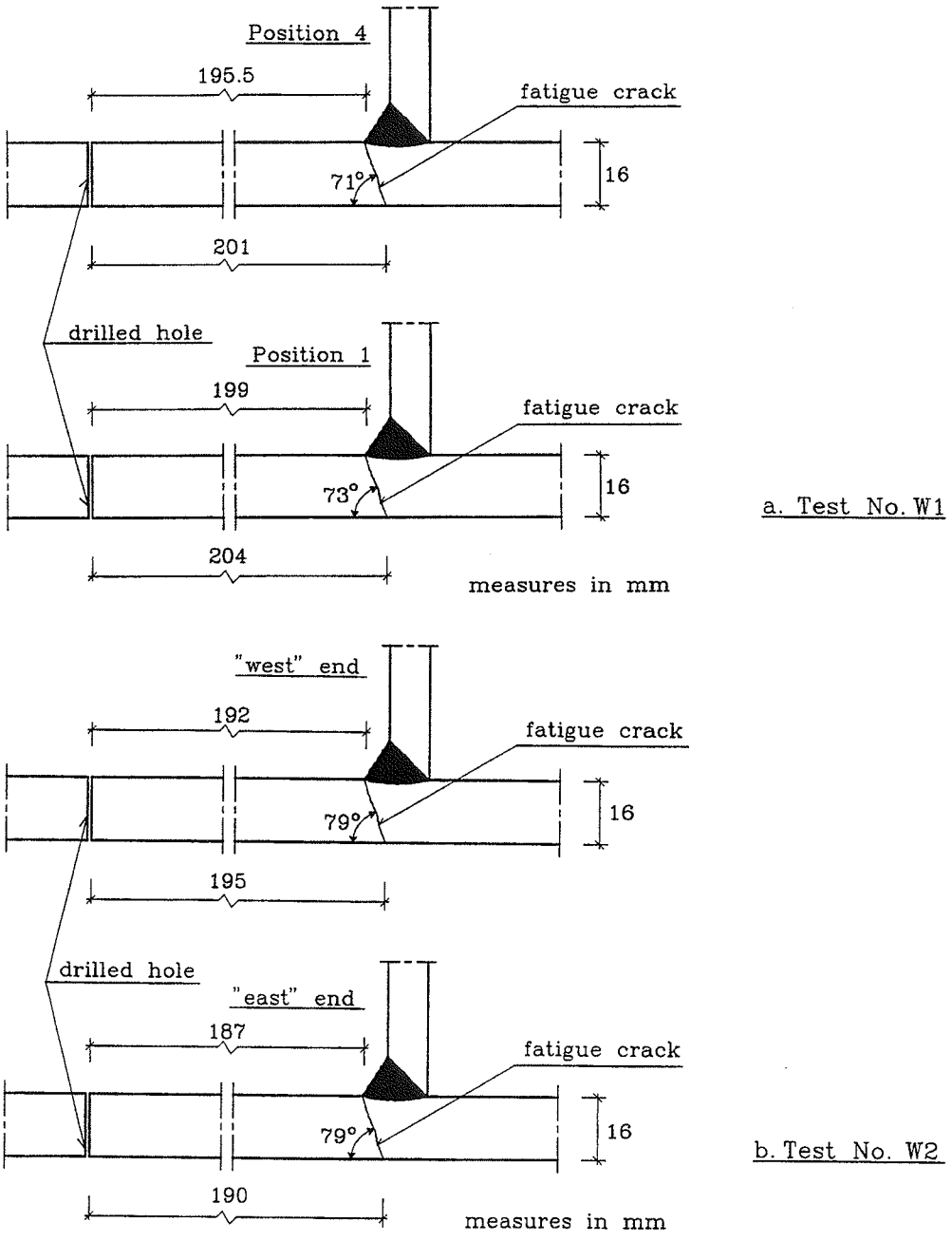

Fig. 4.12 Crack development in main tube wall.

Fig. 4.13 shows the fatigue crack on the interior surface of the chord wall after completion of the fatigue test on test specimen No. W1 ("east" end).

The crack development pattern is reflected in the hot spot stresses at the crown. Figs. 3.4-3.5 show that the hot spot stress is unaffected by the development of fatigue cracks away from the crown. As the cracks grow nearer the crown, the stresses increase rapidly, and when the cracks cross the crown, the stresses decrease almost instantly and change sign. The increase in hot spot stresses is caused by the reduction of the load carrying area, resulting in a stress concentration at the crown.

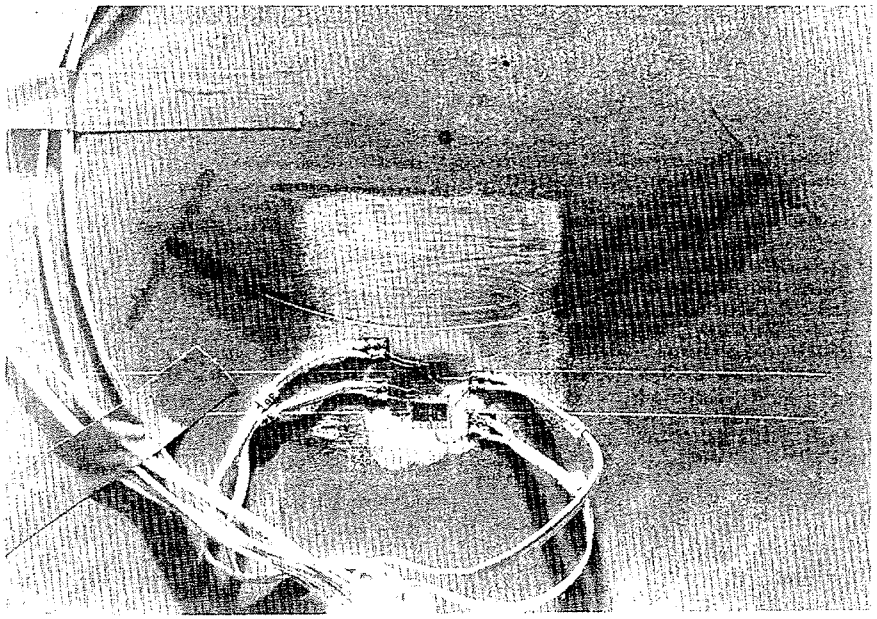

Fig. 4.13 Fatigue crack on interior surface of chord wall. Test No. W1.

5. FATIGUE TEST OBSERVATIONS

When comparing the results obtained in the various test series, it appears that there is a significant difference between constant amplitude and variable amplitude fatigue test results. This could be observed both in the investigations on test specimens in conventional offshore structural steel and in the investigations on high-strength steel. For both the test series on plate test specimens and the series on tubular joints, and with the different load spectra, there is a clear indication that the fatigue life is shorter with variable amplitude loading than with constant amplitude loading for the same stress level.

The difference in fatigue life between constant amplitude and variable amplitude test results is in the following quantified by the Miner sum, M , determined as the number of cycles to failure at variable amplitude loading, N_{va} , divided by the number of cycles to failure at constant amplitude loading, N_{ca} , at the same stress level. When the slope of the linear regression S-N lines from variable amplitude and constant amplitude tests are not identical, M will be a function of the stress level. By using the fitted expressions for the S-N curves, M can be expressed as:

$$M = \frac{N_{va}}{N_{ca}} = \frac{A_{va}}{A_{ca}} \cdot \Delta\sigma^{(m_{ca} - m_{va})} \tag{5.1}$$

In Table 5.1, values of the Miner sum calculated at different stress levels from the regression S-N lines that have been obtained in the present investigation on high-strength steel, are given for the test series on plate specimens with the spectra BROAD64 and PMMOD64. The difference between constant amplitude and variable amplitude test results may also be seen in the S-N diagrams in Figs. 4.3-4.4. It appears from Table 5.1 that the Miner sum corresponding to failure in the variable amplitude test series, varies in the range $\sim$ 0.50-0.80, in all but one case.

The cycle counting method that has been chosen for the analysis of the stress history, "rainflow counting", is usually recommended for broad band loading, [14]. Compared to simple range counting, rainflow counting will give more large cycles when used on a broad band spectrum, whereas the two methods with narrow band loading will yield practically the same result. The difference means that the Miner sum in broad band loading will be even lower by using simple range counting, compared to rainflow counting.

Spectrum	Size of plate test specimens	M		
		$\Delta\sigma$ = 100 MPa	$\Delta\sigma$ = 200 MPa	$\Delta\sigma$ = 300 MPa
BROAD64	Small	0.50	0.52	0.54
	Large	0.63	0.66	0.68
PMMOD64	Small	0.55	0.61	0.65
	Large	0.56	0.81	1.01

Table 5.1 Values of Miner sum, M , at different stress levels, $\Delta\sigma$.

In the similar investigation, [4], on plate test specimens with transverse attachments and in conventional offshore structural steel, it was found that the Miner sum corresponding to failure in general decreases with the irregularity factor of the spectrum. Furthermore, this investigation showed that for the types of load spectra investigated with irregularity factors ranging from ~ 0.7 to 1.00, a more appropriate fatigue damage accumulation formula would be:

$$D = \sum_i \frac{n_i}{N_i} \leq 2 \cdot I - 1 \qquad (5.2)$$

In comparison, the cumulative damage rule generally used in the design of offshore structures today assumes that fracture occurs for a damage ratio of $D = 1$.

In the investigation on high-strength steel plate elements, the spectra used, BROAD64 and PMMOD64, have irregularity factors of $I = 0.75$ and 0.82, respectively. Thus, taking the uncertainties into consideration, it appears from Table 5.1 that the above formula, Eq. 5.2, in general gives a good prediction of the fatigue life for the types of load spectra investigated, also in the case of high-strength steel plate elements.

The S-N lines that have been obtained in the investigation on plate elements in conventional offshore structural steel are given in Ref. 4. A comparison between the resulting S-N lines shows that the high-strength steel plate elements in general have a fatigue life that is ~ 40-120% longer than that of the plate elements in conventional offshore structural steel, depending on the stress level. In only one case - large plate specimens and constant

amplitude loading - no significant difference was observed.

With respect to the tubular joints, the number of test results in the present investigation is too limited to make possible any significant statistical analysis. If best fit S-N lines are determined, assuming a slope of $m = 3$ for both constant amplitude and variable amplitude tests, a Miner sum of $M \sim 0.75$ is found for the variable amplitude tests on the tubular joints in high-strength steel. In the investigation on tubular joints in conventional offshore structural steel, a value of the Miner sum of $M \sim 0.6\text{-}0.8$ was found. With an irregularity factor, $I = 0.82\text{-}0.84$ for the spectra used in the variable amplitude tests on the tubular joints, these results are in good agreement with the observations from the test series on the welded plate test specimens.

If the best fit lines assuming a slope of $m = 3$ are used, the tubular joints in high-strength steel are found to have a fatigue life that is between 0 and 20% longer than that of the joints in conventional offshore structural steel. Figs. 5.1-5.2 show the results that were obtained in the investigations on the tubular joints, both in high-strength steel and in conventional offshore structural steel. With the results obtained for the tubular joints situated within the scatterband from the plate test series, the agreement between the results obtained in the two investigations is considered satisfactory.

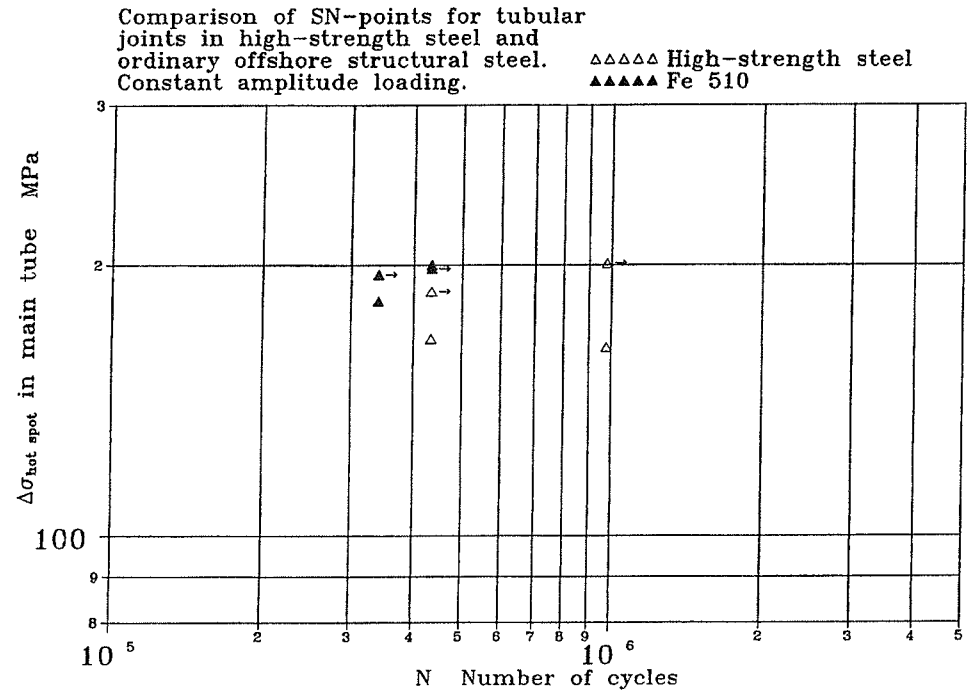

Fig. 5.1 Comparison between results obtained in investigations on full-scale tubular joints. Constant amplitude loading. Stresses in chord.

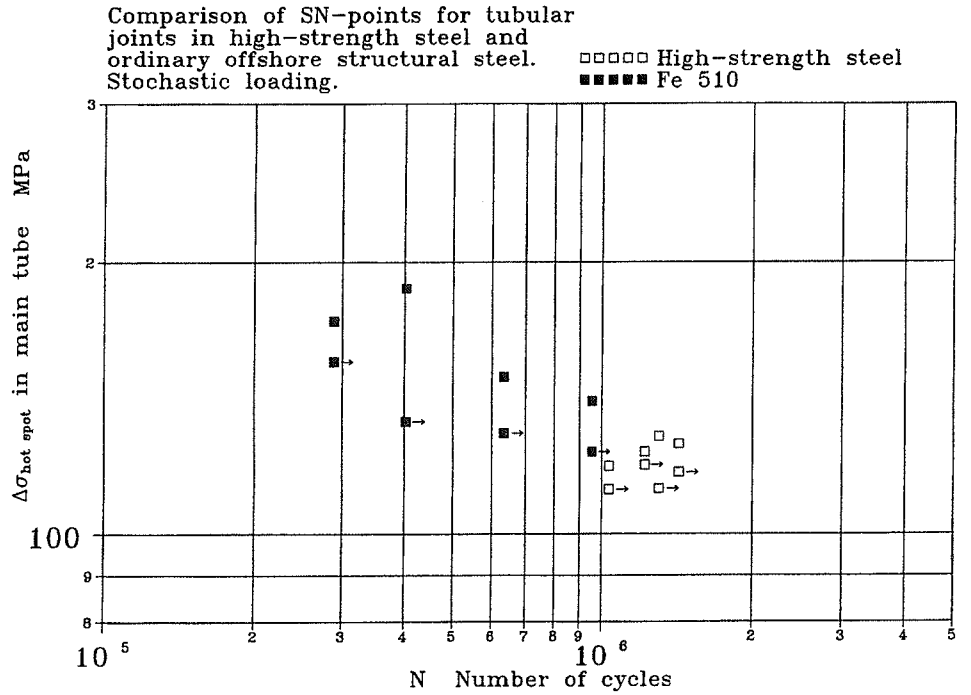

Fig. 5.2 Comparison between results obtained in investigations on full-scale tubular joints. Stochastic loading. Stresses in chord.

6. CONCLUSIONS

In the present investigation, the fatigue life of offshore steel structures under stochastic loading is studied. Of special interest is the problem of fatigue damage accumulation and in this connection, a comparison between experimental results and results obtained using current codes and specifications.

In the load simulation in the variable amplitude fatigue tests, various types of stochastic loading that are realistic in relation to offshore structures have been used. Four different load spectra with irregularity factors ranging from ~ 0.70 to 1.00 have been applied.

The experimental investigation comprises both test series on full-scale tubular joints and test series on smaller welded test specimens. The materials that have been used in the various parts of the investigation have been conventional offshore structural steel, with a yield stress of f_y ~ 360-410 MPa, and high-strength steel with a yield stress, f_y ~ 810-840 MPa.

The present report primarily deals with the results that have been obtained in the investigation on the high-strength steel tubular joints.

The fatigue test series that have been carried through in this investigation show a significant difference between constant amplitude and variable amplitude fatigue test results. For the variable amplitude tests, the stress parameter used is the equivalent constant amplitude stress range, $\Delta\sigma_e$, and the difference between the constant amplitude and variable amplitude test results is quantified by the Miner sum, M, determined as the number of cycles to failure at variable amplitude loading divided by the number of cycles to failure at constant amplitude loading, at the same stress level.

For the welded plate specimens with transverse attachments, more than 250 fatigue tests have been carried out on test specimens in both conventional offshore structural steel and in high-strength steel. It could in all these test series clearly be observed, that the fatigue life is shorter with variable amplitude loading than with constant amplitude loading for the same stress level. The values of the Miner sum that were obtained in the variable amplitude test series on these test specimens, generally vary in the range ~ 0.40-0.85. For the tubular

joints, the number of test results is at present too limited to draw final conclusions. However, the results obtained until now with values of the Miner sum of M $\sim$ 0.6-0.8 for the variable amplitude tests are in good agreement with the results obtained on the plate test specimens.

A comparison of the results obtained in the various test series with variable amplitude loading indicates that the Miner sum decreases with the irregularity factor of the spectrum, and on the basis of these results, a modified fatigue damage accumulation formula is proposed.

For the test series on the welded plate test specimens, it was found that the high-strength steel plate elements in general have a fatigue life that is $\sim$ 40-120% longer than that of the plate elements in conventional offshore structural steel. In only one case, practically the same fatigue life was obtained. For the tubular joint test specimens, the joints in high-strength steel were found to have a fatigue life that is between 0 and 20% longer than that of the joints in conventional offshore structural steel.

7. ACKNOWLEDGMENTS

The present investigation is a part of a larger research program on the fatigue life of offshore steel structures under various types of spectrum loading and under various corrosion conditions. The funding for this investigation has been provided by the Danish Technical Research Council, the Nordic Fund for Technology and Industrial Development, the Technical University of Denmark, and SSAB Oxelösund AB, Sweden, who are gratefully acknowledged.

8. REFERENCES

1. Aarkrog, P.: "A Computer Program for Servo Controlled Fatigue Testing. Documentation and User Guide", Report No. R 253, Dept. of Struct. Engrg., Techn. Univ. of Denmark, 1990.

2. Aarkrog, P., Thorup, E., Krenk, S., Agerskov, H., and Bjørnbak-Hansen, J.: "Apparatur til Udmattelsesforsøg", (Fatigue Test Equipment), in Danish, Report No. R 243, Dept. of Struct. Engrg., Techn. Univ. of Denmark, 1989.

3. Agerskov, H. and Ibsø, J.B.: "Fatigue Life of Repair-Welded Tubular Joints in Offshore Structures", Proceedings of the International Offshore and Polar Engineering Conference, Singapore, pp. 62-69, 1993.

4. Agerskov, H. and Ibsø, J.B.: "Fatigue Life of Plate Elements with Welded Transverse Attachments Subjected to Stochastic Loading", Proceedings of the Nordic Conference on Fatigue. Edited by A.F. Blom, EMAS Publishers, West Midlands, England, 1993.

5. Agerskov, H. and Pedersen, N.T.: "Fatigue Life Prediction of Offshore Steel Structures under Spectrum Loading", International Institute of Welding, Annual Assembly, Haag, 1991, IIW Doc. XIII-1411-91.

6. Agerskov, H. and Pedersen, N.T.: "Fatigue Life of Offshore Steel Structures under Stochastic Loading", ASCE Journ. of Struct. Engrg., Vol. 118, No. 8, pp. 2101-2117, 1992.

7. American Petroleum Institute: "Recommended Practice for Planning, Designing, and Constructing Fixed Offshore Platforms", API RP 2A, 20th ed., Washington, D.C., 1993.

8. Askegaard, V.: "Prediction of Initial Crack Location in Welded Fatigue Test Specimens by the Thermoelastic Stress Analysis Technique", Report No. R 276, Dept. of Struct. Engrg., Techn. Univ. of Denmark, Lyngby, Denmark, 1991.

9. Bogren, J. and Lopez Martinez, L.: "Spectrum Fatigue Testing and Residual Stress Measurements on Non-load Carrying Fillet Welded Test Specimens", Proceedings of the Nordic Conference on Fatigue. Edited by A.F. Blom, EMAS Publishers, West Midlands, England, 1993.

10. British Standards Institution: "Code of Practice for Fixed Offshore Structures", BS 6235, 1982.

11. Christensen, P., Private communications with SSAB Oxelösund, Det Norske Veritas, Copenhagen, Denmark, 1991.

12. Dansk Ingeniørforening: "Norm for Pælefunderede Offshore Stålkonstruktioner", (Code of Practice for the Design and Construction of Pile Supported Offshore Steel Structures), in Danish, Danish Standard DS 449, 1983.

13. Det Norske Veritas: "Rules for the Design, Construction and Inspection of Offshore Structures. Appendix C: Steel Structures", Oslo, Norway, 1982.

14. "Fatigue Handbook. Offshore Steel Structures", Ed.: A. Almar-Næss, Tapir, Trondheim, Norway, 1985.

15. Force Institutes: "6 Stk. Offshore-rørknudesamlinger: Magnetoflux og ultralyd", Rapport 2125010, Copenhagen, Denmark, 1992.

16. Gluver, H.: "One Step Markov Model for Extremes of Gaussian Processes", Report No. R 261, Dept. of Struct. Engrg., Techn. Univ. of Denmark, 1990.

17. Healy, J., Billingham, J., Chubb, J.P., Jones, R.L. and Galsworthy, J.: "Weldable high-strength steels for naval construction", Cranfield Institute of Technology and Defence Research Agency, Holton Heath, Proceedings of the OMAE'93, Conference on Offshore Mechanics and Arctic Engineering, 1993.

18. Ibsø, J.B. and Agerskov, H.: "Fatigue Life of Offshore Steel Structures under Stochastic Loading", Report No. R 299, Dept. of Struct. Engrg., Techn. Univ. of Denmark, Lyngby, Denmark, 1992.

19. Ibsø, J.B. and Agerskov, H.: "Fatigue Life Prediction of Offshore Tubular Structures under Stochastic Loading", Proceedings of the Nordic Conference on Fatigue. Edited by A.F. Blom, EMAS Publishers, West Midlands, England, 1993.

20. Krenk, S. and Gluver, H.: "A Markov Matrix for Fatigue Load Simulation and Rainflow Range Evaluation", Symposium on Stochastic Structural Dynamics, Urbana, Illinois, 1988.

21. Lieurade, H.P. and Wyseur, M.: "Pratique des Essais de Fatigue sur Elements Soudes", International Institute of Welding, Doc. No. XIII-GT1-WG1-17-87,1987.

22. Lopez Martinez, L., Petersen, R.I. and Agerskov, H.: "Fatigue Life of High-Strength Steel Tubular Joints", Proceedings of the Nordic Conference on Fatigue. Edited by A.F. Blom, EMAS Publishers, West Midlands, England, 1993.

23. Lyngkjær, H. and Dahlgren, T.: "Rørknudesamlinger i Offshorekonstruktioner", (Tubular Joints in Offshore Structures), in Danish, M.Sc. Thesis, Dept. of Struct. Engrg., Techn. Univ. of Denmark, 1989.

24. Pedersen, N. Thougård: "Offshorekonstruktioner med Fleksible Knudepunkter", (Offshore Structures with Flexible Joints), in Danish, M.Sc. Thesis, Dept. of Struct. Engrg., Techn. Univ. of Denmark, 1989.

25. Pedersen, N. Thougård and Agerskov, H.: "Fatigue Life Prediction of Offshore Steel Structures under Spectrum Loading", Nordic Steel Colloquium, Odense, September, 1991, pp. 349-362.

26. Pedersen, N. Thougård and Agerskov, H.: "Fatigue Damage Accumulation in Offshore Tubular Structures under Stochastic Loading", International Symposium on Tubular Structures, Delft, pp. 269-280, 1991.

27. Pedersen, N. Thougård and Agerskov, H.: "Fatigue Life Prediction of Offshore Steel Structures under Stochastic Loading", Report No. R 274, Dept. of Struct. Engrg., Techn. Univ. of Denmark, 1991.

28. Petersen, R.I., Agerskov, H., Askegaard, V. and Lopez Martinez, L.: "Fatigue Life of High-Strength Steel Plate Elements with Welded Attachments", Proceedings of the Nordic Conference on Fatigue. Edited by A.F. Blom, EMAS Publishers, West Midlands, England, 1993.

29. Petersen, R.I., Agerskov, H., Lopez Martinez, L. and Askegaard, V.: "Fatigue Life of High-Strength Steel Plate Elements under Stochastic Loading", Report No. R 320, Dept. of Struct. Engrg., Techn. Univ. of Denmark, 1995.

30. Sharp, J.V., Private communications with SSAB Oxelösund, Health & Safety Executive, Offshore Safety Division, London, U.K., 1992.

31. Stanley, P. and Chan, W.K.: "Quantitative stress analysis by means of the thermoelastic effect", J. of Strain Analysis, Vol. 20, (3), pp. 129-137, 1985.

32. Stanley, P. and Chan, W.K.: "A new experimental stress analysis technique of wide application", Proceedings of the VIII'th Int. Conf. on Exptl. Stress Analysis, Amsterdam, The Netherlands, 1986.

33. Vejrum, T. and Nielsen, J.A.: "Udmattelse i Stålkonstruktioner Udsat for Stokastisk Last. Rørknudeforsøg", (Fatigue in Steel Structures Subjected to Stochastic Loading. Tubular Joint Tests), in Danish, M.Sc. Thesis, Dept. of Struct. Engrg., Techn. Univ. of Denmark, Lyngby, Denmark, 1993.

34. Yamada, K. and Agerskov, H.: "Fatigue Life Prediction of Welded Joints Using Fracture Mechanics", Report No. R 255, Dept. of Struct. Engrg., Techn. Univ. of Denmark, 1990.

35. Yamada, K. and Agerskov, H.: "Fatigue Analysis of Plate Elements with Groove Welded Attachments Using Fracture Mechanics", International Institute of Welding, Annual Assembly, Montreal, 1990, IIW Doc. XIII-1365-90.

9. NOTATION

The following symbols are used in this report:

A = constant

a = load level; length; crack depth

b = length

D = damage ratio

d = diameter

F_E, F_G, F_S, F_T, F_W = correction factors

f_u = ultimate tensile strength

f_y = yield stress

I = irregularity factor

$k(\omega)$ = modification factor

M = Miner sum

m = slope of S-N line

N = total number of cycles

n = number of cycles

n_m = number of load levels

P = force

p_{ij} = cumulated transition probability

RMC = root mean cube

RMS = root mean square

$S(\omega)$ = spectral density

SCF = stress concentration factor

T_z = zero upcrossing period

t = thickness

ΔK = stress intensity factor range

$\Delta\sigma$ = stress range

ρ = correlation coefficient

σ = stress; standard deviation; and

ω = angular frequency.